



University
of Glasgow

Guevar, Julien (2016) *Congenital thoracic vertebral malformations in brachycephalic “screw-tailed” dog breeds: Validation of a human classification scheme and a method of Cobb angle measurement in the assessment of vertebral column deformity*. MVM(R) thesis.

<http://theses.gla.ac.uk/7889/>

Copyright and moral rights for this work are retained by the author

A copy can be downloaded for personal non-commercial research or study, without prior permission or charge

This work cannot be reproduced or quoted extensively from without first obtaining permission in writing from the author

The content must not be changed in any way or sold commercially in any format or medium without the formal permission of the author

When referring to this work, full bibliographic details including the author, title, awarding institution and date of the thesis must be given

Glasgow Theses Service

<http://theses.gla.ac.uk/>

theses@gl.a.ac.uk

**CONGENITAL THORACIC VERTEBRAL
MALFORMATIONS IN BRACHYCEPHALIC
“SCREW-TAILED” DOG BREEDS:**

Validation of a human classification scheme and a method
of Cobb angle measurement in the assessment of vertebral
column deformity

Julien Guevar

DVM, MRCVS

Submitted in fulfilment of the requirement for the Degree of
Master in Veterinary Medicine

University of Glasgow

School of Veterinary Medicine

College of Medical, Veterinary and Life Sciences

March 2016

ABSTRACT

Congenital vertebral malformations are common in brachycephalic “screw-tailed” dog breeds such as French bulldogs, English bulldogs, Boston terriers, and Pugs. Those vertebral malformations disrupt the normal vertebral column anatomy and biomechanics, potentially leading to deformity of the vertebral column and subsequent neurological dysfunction. The initial aim of this work was to study and determine whether the congenital vertebral malformations identified in those breeds could be translated in a radiographic classification scheme used in humans to give an improved classification, with clear and well-defined terminology, with the expectation that this would facilitate future study and clinical management in the veterinary field. Therefore, two observers who were blinded to the neurologic status of the dogs classified each vertebral malformation based on the human classification scheme of McMaster and were able to translate them successfully into a new classification scheme for veterinary use.

The following aim was to assess the nature and the impact of vertebral column deformity engendered by those congenital vertebral malformations in the target breeds. As no gold standard exists in veterinary medicine for the calculation of the degree of deformity, it was elected to adapt the human equivalent, termed the Cobb angle, as a potential standard reference tool for use in veterinary practice. For the validation of the Cobb angle measurement method, a computerised semi-automatic technique was used and assessed by multiple independent observers. They observed not only that Kyphosis was the most common vertebral column deformity but also that patients with such deformity were found to be more likely to suffer from neurological deficits, more especially if their Cobb angle was above 35 degrees.

This study has validated the adoption of the human classification scheme and the clinical correlation of the Cobb angle with clinical impact in the study of congenital vertebral malformations in brachycephalic screw-tailed dog breeds.

TABLE OF CONTENTS

Abstract	1
Table of contents	3
List of Tables	5
List of Figures	6
Acknowledgements	10
Author's Declaration	11
Publications and presentations	12
Chapter I CONGENITAL VERTEBRAL MALFORMATIONS IN DOGS: origins and consequences	13
1.1 Embryogenesis and prenatal development of congenital vertebral anomalies and their classification	14
1.1.1 Introduction	14
1.1.2 Embryogenesis and prenatal development	15
1.1.2.1 Approach to the study of the malformations of the vertebral column	23
1.1.2.2 Neural tube defects affecting the vertebral column and spinal cord	24
1.1.2.3 Malformations originating in the embryonic period of development	28
1.1.2.4 Malformations originating in the foetal period of development	31
1.1.3 Classification systems	37
1.2 Deviations of the vertebral column, methods of evaluation and clinical implication	39
1.2.1 Deviations of the vertebral column	39
1.2.2 Methods of evaluation of the curvature deformity	41
1.2.3 Clinical implication	43
1.3 Hypotheses and aims	45
Chapter II MATERIAL AND METHODS	47
2.1 Population and neurological status	48
2.2 Identification and classification of the congenital vertebral malformations	48
2.3 Congenital thoracic vertebral malformations and neurological status	51
2.4 Cobb angle measurement method assessment	52
2.5 Cobb angles, spinal deformity and neurological status	54
Chapter III RESULTS	55

3.1	Population and Neurological Status	56
3.2	Identification and classification of the congenital thoracic vertebral malformations 58	
3.3	Congenital thoracic vertebral malformation and neurological status.....	59
3.4	Cobb angle measurement method assessment.....	60
3.5	Cobb angles, spinal deformity and neurological status.....	61
Chapter IV DISCUSSION		63
4.1	Population and neurological status.....	64
4.2	Identification and classification of the congenital thoracic vertebral malformations 65	
4.3	Congenital thoracic vertebral malformations and neurological Status	67
4.4	Cobb angle measurement method assessment.....	68
4.5	Cobb angles and neurological status	69
4.6	Conclusions	70
List of references.....		73

LIST OF TABLES

Table 1 Some of the main players of the somite differentiation (Fgf, Wnt and Notch signalling pathway). Adapted from Carlson 2014.	19
Table 2 Incidence, breed, sex and age of the population. EB: English bulldog, FB: French bulldog, BT: Boston terrier and SD: Standard deviation. Reprinted with permission from Guevar et al. 2014.	57
Table 3 Clinical 0 to 5 grading scale for thoracolumbar spinal cord lesions (Sharp & Wheeler 2005) and incidence in the two groups. Reprinted with permission from Guevar et al. 2014.	57
Table 4 Number of vertebrae affected by each type of congenital vertebral malformation in dogs with associated neurological deficits (group 1) and dogs without associated neurological deficits (group 2). A significant difference in the types of congenital vertebral malformations was evident when comparing the two groups ($P = 0.01$) reprinted with permission from Gutierrez-Quintana et al. 2014.	60
Table 5 Intraclass correlation coefficient (ICC) and 95% confidence intervals (CI) for digital measurement of the Cobb angles. 1,2,3: refer to the 3 observers reprinted with permission from Guevar et al. 2014.	60

LIST OF FIGURES

- Figure 1 Gastrulation. The bilaminar embryonic disc surrounded by the amnion and yolk sac (Left). During gastrulation, a trilaminar disc forms from the bilaminar disc creating the model for the future ectoderm, mesoderm and endoderm (Right). Reprinted with permission from (Kaplan et al. 2005) 15
- Figure 2 Notochord formation and mesoderm differentiation. The notochordal plate folds into the notochord after which the mesoderm surrounding this structure differentiates into the paraxial, intermediate and lateral mesoderms. Reprinted with permission from (Kaplan et al. 2005)..... 16
- Figure 3 Transverse view of the neural tube, notochord, paired aortae, and somites consisting of myotome and sclerotome. Reprinted with permission from Vosbikian et al. 2011..... 17
- Figure 4 Resegmentation theory illustration. (A) View of sclerotomes around the notochord separated by arteries located between segments. (B) Resegmentation of the sclerotomes into rostral and caudal portions. (C) Formation of the centrum from the fusion of adjacent sclerotomes. (D) Further development into the early vertebral body and intervertebral disk. Reprinted with permission from Vosbikian et al. 2011..... 18
- Figure 5 Diagram of the two Pax gene expressed in sclerotomes (Pax gene family). Location on human chromosomes, sites of expression, and known effects in human and mouse. The structures of conserved elements of these genes are schematically represented; KO, knockout. Reprinted with permission from Carlson 2014. 18
- Figure 6 *Hox* gene expression in relation to the development of the vertebral column of the mouse. The vertebral column of the mouse (left) has one more thoracic and one more lumbar vertebra than the vertebral column of the human. Green asterisks indicate levels at which there is definite expression of the *Hox* gene indicated at the top of the column. Purple circles represent the caudal border where expression fades out. Tan circles represent areas of no expression of the *Hox* gene. Reprinted with permission from Carlson 2014....21
- Figure 7 Phases of somitogenesis in a stage 12 chick embryo and possible causal links between teratogen target tissues and hypothesised mature dysmorphogenesis. Reprinted with permission from Alexander & Tuan 2010.23
- Figure 8 Dorsoventral radiograph of a Pug with scoliosis, congenital vertebral malformations including spina bifida (black circle).24
- Figure 9 Open spinal dysraphism in a puppy. A. Fissure consistent with open spina bifida in the entire lumbosacral region in a stillborn mongrel dog. B. Ventrodorsal plain radiographs of the vertebral column revealed a defect in the fusion of the dorsal spinous processes of the L4, L5, L6 L7 and sacral vertebrae. C and D. Dorsal view of vertebral column after maceration. Vertebral arches of C2, C7 and T1 were partially open. Opening

in the lumbar and sacral vertebrae was confirmed. Reprinted with permission from Arias et al. 2008.....	25
Figure 10 Cat with myelomeningocele with tethered spinal cord syndrome. Markers on the skin indicate the cranio-caudal extent of the cutaneous mass. Sagittal and transverse T1-weighted (A,B) and T2-weighted images (C,D). There is a communication between the subarachnoid space and the cutaneous mass through a defect of the dorsal lamina in a cat with myelomeningocele with tethered spinal cord syndrome. Reprinted with permission from Ricci et al. 2011.....	26
Figure 11 Cross section of the spinal cord and adjacent structures at various levels in a Manx cat: cranial lumbar area (top left) with cavity in dorsal funiculi, middle lumbar cord (top right) with enlarged cavity in dorsal funiculi, caudal lumbar cord (bottom left). The cavity is now confluent with the central canal and sacral cord (bottom right). The cord is flattened dorsoventrally. The lesion is separated from the central canal and is covered dorsally by ectoderm. Thionin stain. Reprinted with permission from Martin 1971.....	27
Figure 12 Schematic illustration of the pairing defect of sclerotomic cells as a result of asynchronous development of hemimetameric pair. If the paired somite derivatives are not in the same developmental phase by the time of midline fusion, the tardy side may shift one segment caudad. At the level of initial discrepancy a solitary hemivertebra develops. This is believed by the authors to be the most common mechanism of hemivertebra formation. Reprinted with permission from Tsou et al. 1980.....	29
Figure 13 Hemivertebrae variations: (A) Double balanced hemivertebra. Two asynchronous pairs deployed tardy hemimetamer on contralateral sides. (B) Solitary hemivertebra as a result of asynchronous development of hemimetameric pair. Reprinted with permission from Tsou et al. 1980.	30
Figure 14 Hemimetamer hypoplasia and aplasia: (A) Hemimetamer hypoplasia, mild. (B) Single hemimetamer aplasia, solitary hemivertebra. The medial border of this type of hemivertebra is irregular and crosses the midline. Contralateral rib fragments may persist. Reprinted with permission from Tsou et al. 1980.....	31
Figure 15 The wavefront: consisting of opposing gradient of retinoic acid (RA) and fibroblast growth factor-8 (FGF). Reprinted with permission from Carlson 2014.....	32
Figure 16 The segmentation clock: oscillation of molecules in the Notch pathway stimulates the expression of lunatic fringe at the anterior and c-hairy at the posterior border of a future somite. Later, interactions between Eph A and Ephrin B maintain the intersomitic space. Reprinted with permission from Carlson 2014.	33
Figure 17 Centrum hypoplasia and aplasia, five common patterns seen in humans (a-e): a, wedge; b, posterior hemicentrum; c, lateral hemicentrum; d, posterior quadrant centrum; e, centrum aplasia. The posterior corner hemivertebra of Risser (f) is primarily an embryonic anomaly of asynchronous development of hemimetamer pair. The unpaired hemivertebra lateral centrum half suffers further anterior growth disturbance during the foetal period.	

The residue posterior quadrant centrum is accompanied by ipsilateral hemiarch in contrast to the intact neural arch of posterior quadrant centrum (d). Reprinted with permission from Tsou et al. 1980.	35
Figure 18 Schematic diagram of proposed classification of congenital vertebral anomalies in humans. All anomalies (excluding primary neural tube closure defects and occipito-C1-C2, malformations) are initially divided into two main groups, embryonic and foetal, according to the time of origin during gestation of each anomaly. Common pathogenesis guides the subsequent groupings. The specific anatomic defect is emphasized. Reprinted with permission from Tsou et al. 1980.	36
Figure 19 Classification system of Nasca et al (1975) used in veterinary medicine for five clinical cases. Reprinted with permission from Besalti et al. 2005.	38
Figure 20 McMaster classification for vertebral anomalies. Drawings showing the different types of vertebral anomalies that produce a congenital kyphosis or kyphoscoliosis. Reprinted with permission from McMaster & Singh 1999.	38
Figure 21 Reconstructed sagittal CT of a dog with a thoracic vertebral malformation. Mid-sagittal plane (A) and transverse plane at T5 (B) and T9 (C) highlighting the progressive narrowing of the vertebral canal.	40
Figure 22 Sagittal T2 weighted MRI of the thoracic spine showing a T9 vertebral malformation and secondary kyphosis. Transverse T2 weighted MRI at the level of (A) and caudal to (B) the vertebral malformation highlighting the spinal cord compression.	41
Figure 23 Schematic line drawing showing the radiographic appearance of the vertebral malformation classification system used in this study. Reprinted with permission from Gutierrez-Quintana et al. 2014.	49
Figure 24 Congenital vertebral malformations identified on lateral radiographs of the thoracic vertebral column. (A) Block vertebrae, where there is failure of normal segmentation of the vertebrae, evident as the failure of division of T8 and T9 vertebral bodies (open arrow) and spinous process (solid arrow). (B) Ventral hypoplasia of T8 vertebral body (ventral wedge shape vertebra) (arrow) with kyphosis. (C) Ventral aplasia of T8 vertebral body (dorsal hemivertebra) (arrow) with more severe kyphosis. Reprinted with permission from Gutierrez-Quintana et al. 2014.	50
Figure 25 Congenital vertebral malformations identified on ventro-dorsal radiographs of the thoracic vertebral column. (A) Ventral hypoplasia of T8 vertebral body (arrow, this is the same case as figure 2B): no evidence of scoliosis is evident on the ventro-dorsal view if there is no lateral hypoplasia. (B) Ventro-lateral aplasia of T8 vertebral body (dorso-lateral hemivertebra) (arrow). This case had similar changes to figure 2C on the lateral view. (C) Ventral and median aplasia of the vertebral body (Butterfly vertebra) (arrow). Reprinted with permission from Gutierrez-Quintana et al. 2014.	51
Figure 26 Cobb angles measurements. Lateral and ventro-dorsal radiographs of a neurologically normal Pug with a congenital vertebral malformation at the eighth thoracic	

vertebra (T8) identified as an incidental finding (A,C) and a clinically affected Pug with a related congenital vertebral malformation at the seventh thoracic vertebra (T7) (B,D). The placement of the reference lines for the calculation of the kyphotic (lateral radiograph) and scoliotic (ventro-dorsal radiograph) angles is shown. The lines pass over the cranial vertebral end plate of T7 and over the caudal vertebral end plate of the ninth thoracic vertebra (T9) in the normal Pug (A,C); and similarly over the vertebral end plates of the sixth thoracic vertebra (T6) and T8 in the affected Pug (B,D). Reprinted with permission from Guevar et al. 2014.53

Figure 27 Histogram showing the frequency of defects of vertebral body formation by vertebral column level. For clarity, the unclassified vertebral malformations (n=35) were not included in this graph. Reprinted with permission from Gutierrez-Quintana et al. 2014.59

Figure 28 Boxplots of the kyphotic Cobb angles for group1 and group 2 (2a) ($P=0.0006$) and boxplots of the scoliotic angles of groups 1 and 2 (2b) ($P=0.5462$) reprinted with permission from Guevar et al. 2014.62

Figure 29 Schematic line drawings of the short vertebra: showing the radiographic appearance of the additional vertebral malformation found frequently in this study: symmetrical hypoplasia of the vertebral body (“short” vertebra) reprinted with permission from Gutierrez-Quintana et al. 2014.66

ACKNOWLEDGEMENTS

I would like to thank my supervisors, Rodrigo Gutierrez-Quintana and Professor James Anderson, for their support and guidance in accomplishing this work.

I would also like to thank Jacques Penderis for his inspiring mentorship and Catherine Stalin for her support in my residency program.

I would like to thank the other members of the neurology team Kiterie Faller, Carmen Yeaman and Karen Bell for keeping me in the right track when my mind went on a wonder.

I would also like to thank Tim Parkin for his help with statistical analysis in the two publications as well as Mikael Grevitt from the Centre for Spine Studies and Surgery at Nottingham University hospitals for his review of the second publication.

Finally, I would like to thank the imaging and anaesthesia departments for their help in acquiring the data for this work and the nursing staff for looking after the patients.

AUTHOR'S DECLARATION

The work presented in this thesis was performed by the author with close collaboration with one of the supervisors Rodrigo Gutierrez-Quintana, except where the assistance of others has been acknowledged.

Julien Guevar, September 2016

PUBLICATIONS AND PRESENTATIONS

Gutierrez-Quintana, R., Guevar, J., Stalin, C., Faller, K., Yeamans, C. and Penderis, J. (2014). A proposed radiographic classification scheme for congenital thoracic vertebral malformations in brachycephalic “screw-tailed” dog breeds. *Veterinary Radiology & Ultrasound*, 55: 585–591. doi: 10.1111/vru.12172

An abstract with limited preliminary results of this study was submitted to the European College of Veterinary Neurology Annual Symposium, September 2013, Paris, France.

Guevar, J., Penderis, J., Faller, K., Yeamans, C., Stalin, C., & Gutierrez-Quintana, R. (2014). Computer-assisted radiographic calculation of spinal curvature in brachycephalic “screw-tailed” dog breeds with congenital thoracic vertebral malformations: reliability and clinical evaluation. *PloS one*, 9(9), e106957.

An abstract with limited preliminary results of this study was submitted to the European College of Veterinary Neurology Annual Symposium, September 2013, Paris, France.

**CHAPTER I CONGENITAL VERTEBRAL
MALFORMATIONS IN DOGS: ORIGINS AND
CONSEQUENCES**

1.1 Embryogenesis and prenatal development of congenital vertebral anomalies and their classification

1.1.1 Introduction

The exact incidence of congenital malformations of the axial skeleton affecting dogs and cats has not been reported. Congenital malformations affecting the vertebrae are well-recognised entities in veterinary medicine and are, not uncommonly, identified as incidental findings during unrelated diagnostic imaging investigation (Dewey & da Costa 2016). Congenital malformations of the vertebral column alter the normal anatomy and therefore its biomechanics leading to deformities but also pain, myelopathy and radiculopathy (Westworth & Sturges 2010).

Although it is reported that breed predispositions exist for the various congenital malformations, the aetiology for those predispositions is unclear in small animal (Dewey et al. 2015). Though the incidence of congenital vertebral malformations in dogs is unknown, there is a clear predisposition to so-called screw-tailed dog breeds such as Pugs, French and English bulldogs and Boston terriers, where the tail anatomical variation makes it look like a screw (Westworth & Sturges 2010; Dewey & da Costa 2016; Schlensker & Distl 2016). In comparison, it is known in man that approximately 1/1000 live births are afflicted with an axial skeleton defect (Alexander & Tuan 2010).

Typically, when discussing congenital abnormalities of the vertebral column, the classification of the defects is divided in three main categories, which refer to stages of development. They are neural tube defects, defects of segmentation and lastly defects of formation. Therefore, understanding the normal development of the vertebral column is essential when trying to pinpoint what, where and when an error occurred.

1.1.2 Embryogenesis and prenatal development

Although a detailed review of the embryology is beyond the scope of this work, an overview of the embryology of the vertebral column is pertinent to understanding the various congenital malformations, which are further described in this study. It is well-known that the notochord and somites are the most important structures involved in the development of the future vertebral column (Kaplan et al. 2005) and their origin and development is described below. The neural development however will not be reviewed.

The early embryological origin of the vertebral column begins during the period known as the gastrulation. It is a process during which a bilaminar embryonic disc differentiates into a trilaminar disc (Figure 1). The primitive streak, a well-defined germ layer, and the notochord develop during that period. The formation of important structures such as the neural tube, the notochord and the mesoderm follow.

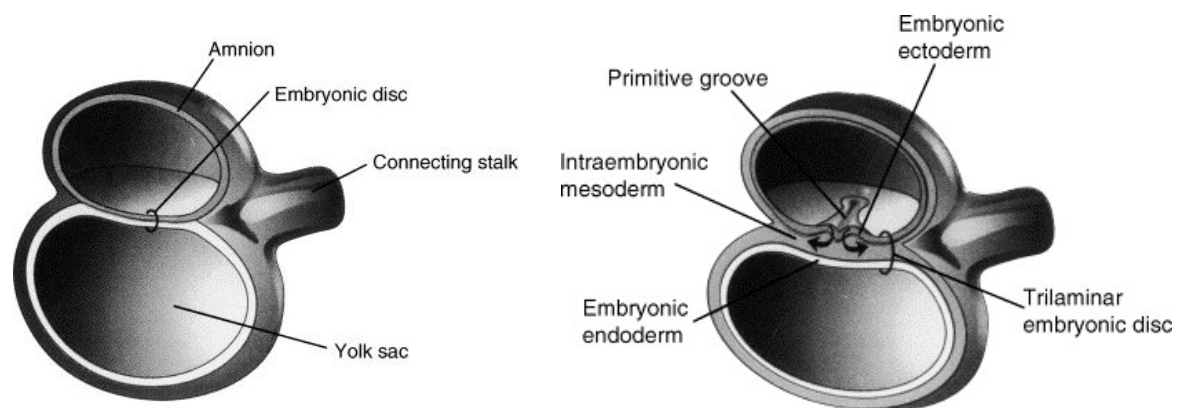


Figure 1 Gastrulation. The bilaminar embryonic disc surrounded by the amnion and yolk sac (Left). During gastrulation, a trilaminar disc forms from the bilaminar disc creating the model for the future ectoderm, mesoderm and endoderm (Right). Reprinted with permission from (Kaplan et al. 2005)

The notochord arises from the infolding of the notochordal plate and will contribute to the elaboration of the nucleus pulposus of the intervertebral disc. More recently, it has been suggested that the notochord may also play a part in the vertebral patterning (Fleming et al.

2004). On both sides of the notochord, the mesoderm differentiates into three areas: paraxial, intermediate and lateral mesoderms (Figure 2).

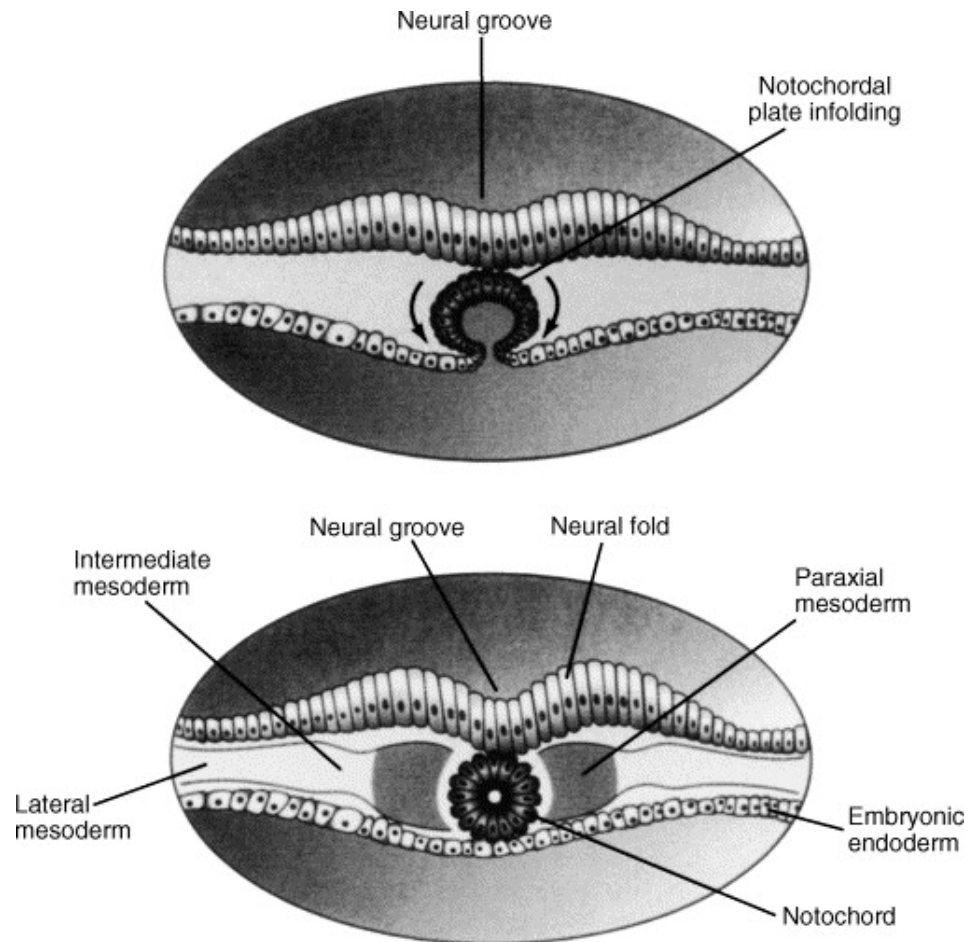


Figure 2 Notochord formation and mesoderm differentiation. The notochordal plate folds into the notochord after which the mesoderm surrounding this structure differentiates into the paraxial, intermediate and lateral mesoderms. Reprinted with permission from (Kaplan et al. 2005).

Further differentiation of the paraxial mesoderm develops into pairs of somites. The formation of somites is a spatially and temporally regulated formation that occurs through cyclic oscillation of genes called the somite segmentation clock, involving various signalling molecules, factors and pathways such as Wnt, Fgf and Notch signalling pathways (Mead & Yutzey 2012) further explained in

Table 1 (page 19) and section 1.1.2.4 (page 31) . The somites differentiate into two major regions. The first one is dorsolateral and gives rise to the dermatome and myotome, which

will eventually mature into skin dermis and spinal musculature. The second one is ventromedial and is named the sclerotome, from which the vertebral column matures (Vosbikian et al. 2011) (**Figure 3**). The elaboration of the sclerotome is induced by the notochord (via sonic hedgehog) on the somite (Carlson 2014). The annulus fibrosus of the intervertebral disc will come from the proliferating sclerotome.

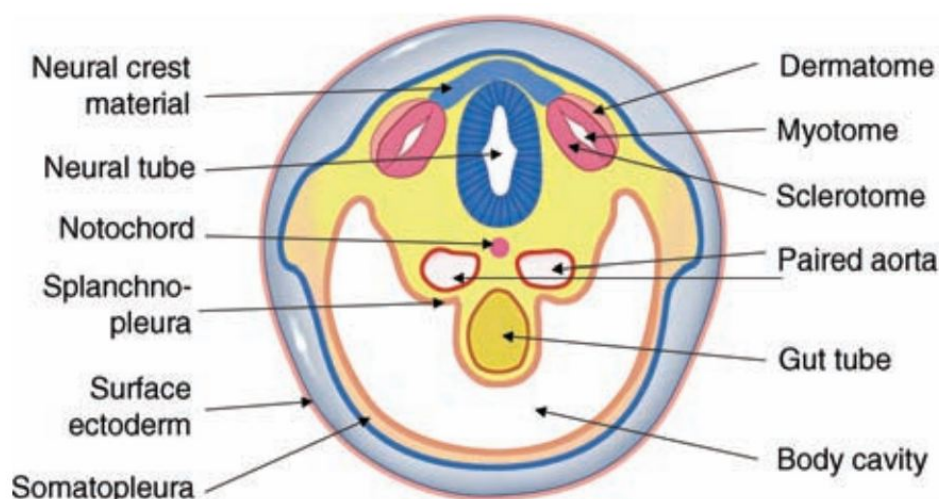


Figure 3 Transverse view of the neural tube, notochord, paired aortae, and somites consisting of myotome and sclerotome. Reprinted with permission from Vosbikian et al. 2011.

The theory of the resegmentation, in which a sclerotome splits into a cranial and a caudal half, is a key step in the development of the vertebral column. The development of an individual vertebra therefore comes from the union of the caudal half of a sclerotome with the cranial half of the adjacent sclerotome. This leads to the formation of the centrum of the vertebra, which will eventually become the vertebral body and the formation of the dorsal part of the vertebra, the neural arch (**Figure 4**).

The formation of the centrum is under the continuing influence of sonic hedgehog (Shh), influencing the expression of *Pax-1*, a member of the Pax gene family, expressed at the level of the sclerotome. A mutation of the latter gene has the potential to lead to vertebral malformations in humans ((Carlson 2014);**Figure 5**). The development of the neural arch

is coordinated by another set of developmental controls with the expression of Pax-9 and the homeobox-containing genes *Msx-1* and *Msx-2*, which guide the cells of the dorsal sclerotome to form the neural arch (Carlson 2014); **Figure 5**; Table 1)

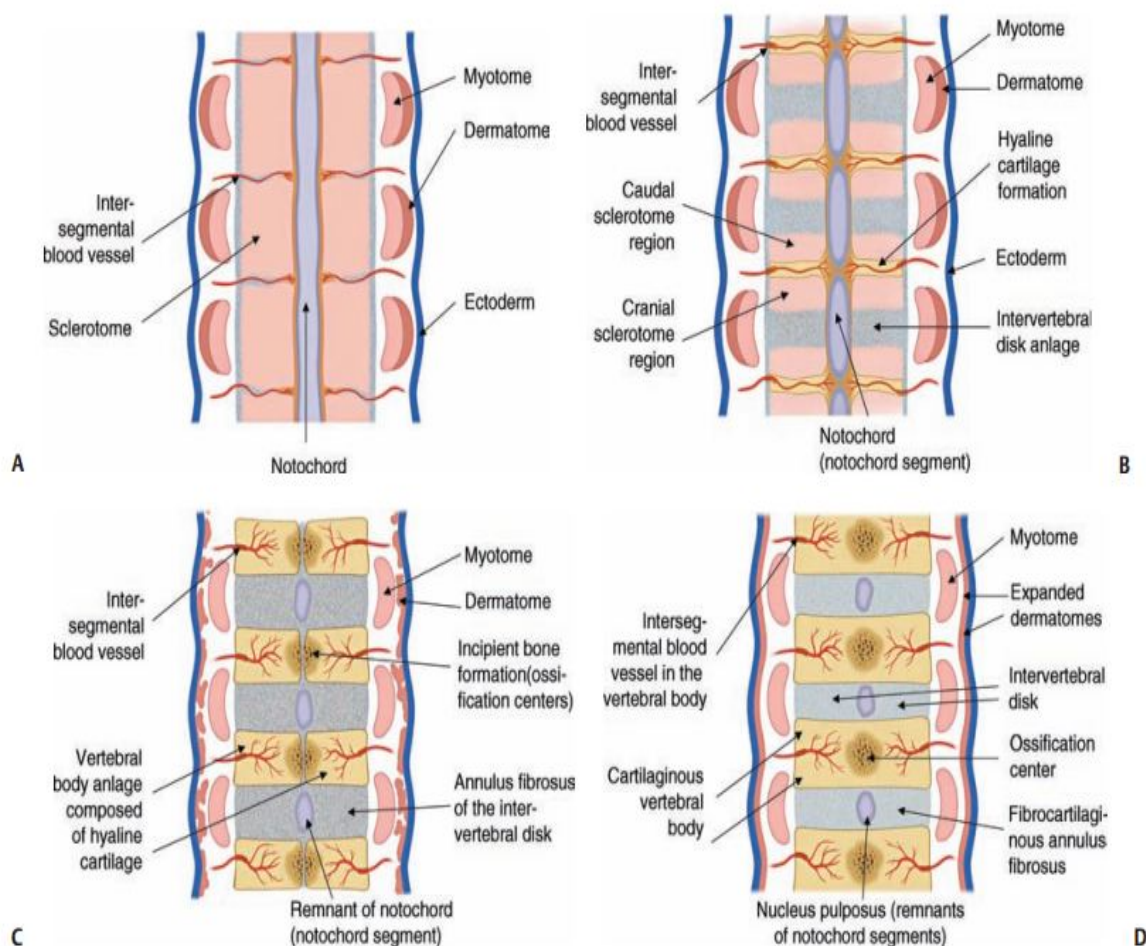


Figure 4 Resegmentation theory illustration. (A) View of sclerotomes around the notochord separated by arteries located between segments. (B) Resegmentation of the sclerotomes into rostral and caudal portions. (C) Formation of the centrum from the fusion of adjacent sclerotomes. (D) Further development into the early vertebral body and intervertebral disk. Reprinted with permission from Vosbikian et al. 2011.

Gene	Chromosomal localization					Sites of expression	Mutants	
	Human	N	PD	Oct	HD		Mouse	Human
Pax-1	20p11					Sclerotome, perivertebral mesenchyme, thymus	<i>Undulated</i> (un)	Vertebral malformations
Pax-9	14q12-q13					Sclerotome, perivertebral mesenchyme	KO: oligodontia	Oligodontia

Figure 5 Diagram of the two Pax gene expressed in sclerotomes (Pax gene family). Location on human chromosomes, sites of expression, and known effects in human and mouse. The structures of conserved elements of these genes are schematically represented; KO, knockout. Reprinted with permission from Carlson 2014.

	Further information
Fgf (Fibroblast growth factor) family	Fibroblast growth factor (FGF) was initially described in 1974 as a substance that stimulates the growth of fibroblasts in culture. Since then, the originally described FGF has expanded into a family of 22 members, each of which has distinctive functions. Many members of the FGF family play an important role in a variety of phases of embryonic development and in fulfilling functions, such as the stimulation of capillary growth, in the post natal body.
Wnt Family	The Wnt family of signalling molecules is complex, with 18 members represented in the mouse. Related to the segment-polarity gene <i>Wingless</i> in <i>Drosophila</i> , Wnts play dramatically different roles in different classes of vertebrates. In amphibians, Wnts are essential for dorsalization in the very early embryo, whereas their role in preimplantation mouse development seems to be minimal. In mammals, Wnts play many important roles during the period of gastrulation. As many organ primordia begin to take shape, active Wnt pathways stimulate the cellular proliferation that is required to bring these structures to their normal proportions. Later in development, Wnts are involved in a variety of processes related to cellular differentiation and polarity.
Notch signalling pathway	The Notch signalling pathway is a short-range communication transducer that is involved in regulating many cellular processes (proliferation, stem cell and stem cell niche maintenance, cell fate specification, differentiation, and cell death) during development and renewal of adult tissues. Notch signalling is mediated by proteolysis and does not appear to involve any secondary messengers. However, depending on cellular context, the amplitude and timing of Notch activity can be regulated by posttranslational modifications to ligands and receptors and their trafficking.
<i>Msx</i> genes	The <i>Msx</i> genes (homologous to the muscle –segment homeobox (<i>msh</i>) gene in <i>drosophila</i>) constitute a small, highly conserved family of homeobox-containing genes, with only two representatives in humans. Nevertheless, the <i>Msx</i> proteins play important roles in embryonic development, especially in epitheliomesenchymal interactions in the limbs and face. <i>Msx</i> proteins are general inhibitors of cell differentiation in prenatal development, and in postnatal life they maintain the proliferative capacity of tissue.

Table 1 Some of the main players of the somite differentiation (Fgf, Wnt and Notch signalling pathway). Adapted from Carlson 2014.

The regional characteristics of the vertebrae (atlas, axis, cervical, thoracic, lumbar regions, etc.) are variable along the vertebral column. Those characteristics are specified by the actions of discrete combinations of homeobox-containing genes (Carlson 2014). A unique combination of Hox genes leads to the formation of the normal segmental pattern along the craniocaudal axis of the vertebral column. For example, the expression of four genes (Hoxa1, Hoxa3, Hoxb1, Hoxd4) leads to the formation of the axis whereas formation of the atlas has the same four genes plus 2 others (Hoxa4 and Hoxb4), in the mouse model. The *Hox* gene expression in relation to the development of the vertebral column of the mouse is illustrated in **Figure 6** (page21).

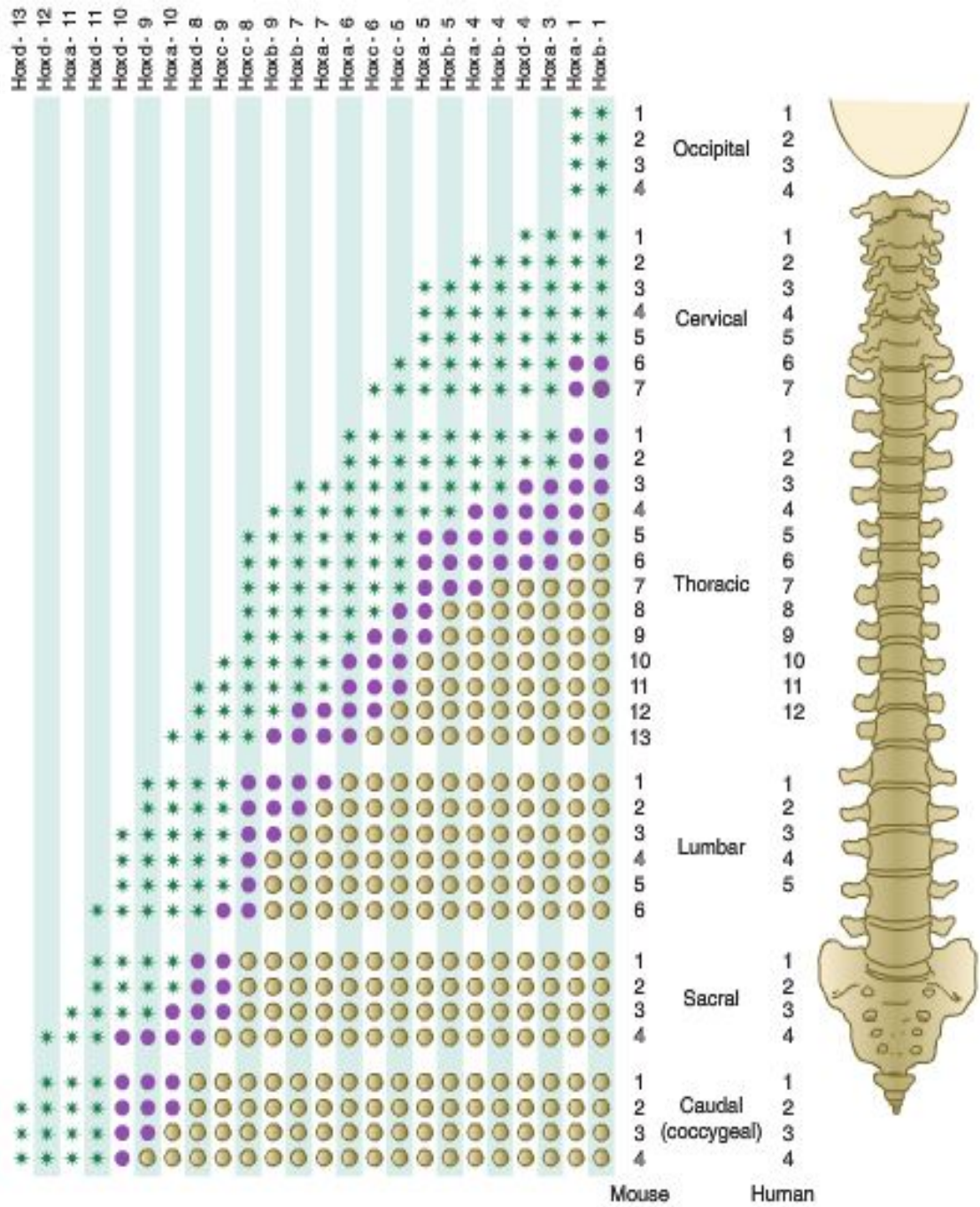


Figure 6 *Hox* gene expression in relation to the development of the vertebral column of the mouse. The vertebral column of the mouse (left) has one more thoracic and one more lumbar vertebra than the vertebral column of the human. Green asterisks indicate levels at which there is definite expression of the *Hox* gene indicated at the top of the column. Purple circles represent the caudal border where expression fades out. Tan circles represent areas of no expression of the *Hox* gene. Reprinted with permission from Carlson 2014.

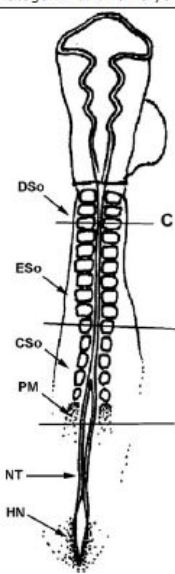
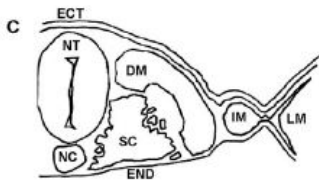
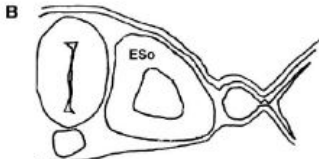
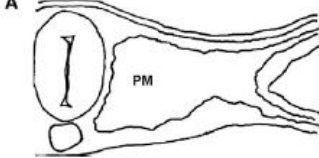
Finally, the centrum and the two halves of the vertebral arches develop separately and must therefore fuse to one another. After chondrification, ossification will begin and the notochord disintegrates. This complex, multi-step and highly regulated process of skeletogenesis takes place under the influence of several cell signalling pathways amongst which the important Notch pathway (Mead & Yutzey 2012).

In such a multifactorial environment, any abnormalities affecting the mesenchyme, the notochord or genetic factors may affect the aforementioned signalling pathways and predispose to an abnormal development of the bony skeleton (Nolting et al. 1998; Kaplan et al. 2005). Individual or combinations of defects are possible. Metabolic diseases, particularly folate, teratogenous drugs and toxin exposure have all been incriminated as potential aetiologies (Summers et al. 1995; Westworth & Sturges 2010).

It is likely that there is a time-dependent, tissue-specific insult upon the skeletal component underlying the abnormal development (Figure 7) (Alexander & Tuan 2010). It is interesting to highlight the influence of hypoxia as an environmental teratogenic factor, especially in the context of brachycephalic breeds affected by respiratory issues. Transient hypoxic conditions during the embryonic period increase the incidence of congenital vertebral anomalies (Alexander & Tuan 2010).

If a congenital vertebral malformation has been identified, screening for other associated anomalies of the nervous system and other systems (i.e. cardiopulmonary, genitourinary, gastrointestinal, and skeletal) should be done as they may be concurrent (Westworth & Sturges 2010). This is supported by the results reported by Jaskwicz et al (2000) that anomalies occur at sites other than the spine in 30% to 60% of children with congenital spinal anomalies. This may simply be explained by the close spatial developmental relationship, which exists between their mesodermal precursors (leading to the development of spinal column, urogenital system and gut cavity). The various syndromes

where congenital vertebral malformations are implicated and reported in human medicine are not reviewed.

Stage 12 chick embryo	Transverse section/time of teratogenic insult	Target tissue	Possible resultant dysmorphogenesis
		<ol style="list-style-type: none"> 1. Notochord 2. Ectoderm/neural tube 3. Sclerotome 	<ul style="list-style-type: none"> Cleft vertebrae Vertebral element agenesis Vertebral disc anomalies and abnormal bone metabolism
		<ol style="list-style-type: none"> 1. Notochord 2. Ectoderm/neural tube 3. Somitic mesoderm 4. Lateral plate mesoderm 	<ul style="list-style-type: none"> Cleft vertebrae Vertebral agenesis Hemivertebrae and block vertebrae Fused ribs and bifid ribs
		<ol style="list-style-type: none"> 1. Chordamesoderm/notochord 2. Paraxial mesoderm 3. Ectoderm 	<ul style="list-style-type: none"> Vertebral disc anomalies and caudal agenesis Vertebral agenesis and hemiblock vertebrae Block or hemivertebrae bifid or fused ribs vertebral agenesis

Labels: DSo, differentiated somite; ESo, epithelial somite; CSo, condensed somite; PM, paraxial mesoderm; NT, neural tube; HN, Hensen's node; ECT, ectoderm; END, endoderm; NC, notochord; DM, dermomyotome; SC, sclerotome; IM, intermediate mesoderm; LM, lateral plate mesoderm.

Figure 7 Phases of somitogenesis in a stage 12 chick embryo and possible causal links between teratogen target tissues and hypothesised mature dysmorphogenesis. Reprinted with permission from Alexander & Tuan 2010.

1.1.2.1 Approach to the study of the malformations of the vertebral column

The study of the malformations of the vertebral column will be divided into three main categories, as explained in the introduction (section 1.1.1, page 14). The first one relates to the primary neural tube defects occurring during development and the two others relate to the anomalies occurring during the embryonic and foetal period respectively. When studying congenital abnormalities, it is important to identify the type of malformation, the resulting deformity and the specific region of the vertebral column involved. In this work, particular attention will be given to the malformations affecting the thoracolumbar segment of the vertebral column.

1.1.2.2 Neural tube defects affecting the vertebral column and spinal cord

A spinal neural tube defect refers to a vertebral column and spinal cord congenital malformation, which is secondary to an abnormal closure of the neural tube at its caudal neuropore during its development (Westworth & Sturges 2010). As a result of the closure abnormality, the midline has a defect through which structures such as neural components or meninges may herniate. Such is the case with spinal dysraphism.

Spinal dysraphism encompasses the group of dorsal midline defects secondary to the abnormal development of ectoderm, mesoderm, and neurectoderm layers of tissue. Spina bifida, meningocele, meningomyelocele, and diastematomyelia are amongst the malformations. In veterinary medicine, they are classified as open or closed, depending on the presence or absence of nervous tissue exposition to the environment. This classification is similar to the one used in humans (**Figure 8**) (Westworth & Sturges 2010).

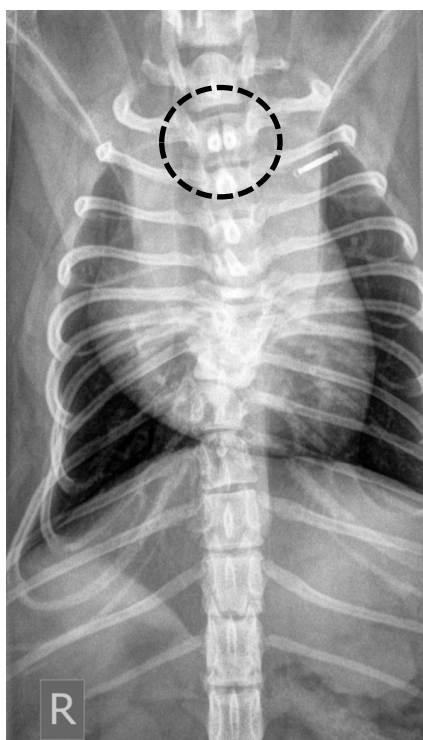


Figure 8 Dorsoventral radiograph of a Pug with scoliosis, congenital vertebral malformations including spina bifida (black circle).

Open spinal dysraphism (spina bifida aperta) such as myeloceles and meningocele are open to the environment, as they are not covered by skin. They have only been rarely reported in dogs or cats (Frye & Mcfarland 1965; Chesney 1973; Clayton & Boyd 1983; Shamir et al. 2001; Arias et al. 2008). **Figure 9** shows the clinical, radiographic and post-mortem findings of this condition in a stillborn dog.

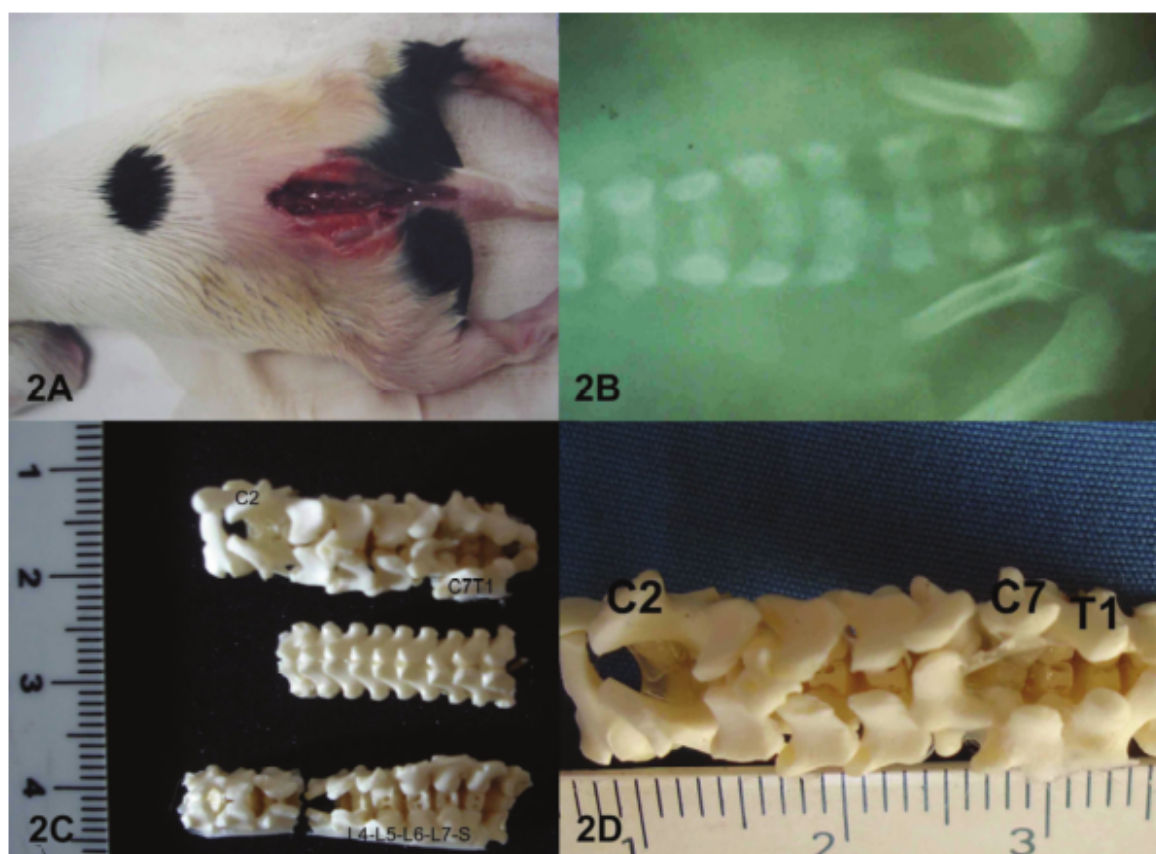


Figure 9 Open spinal dysraphism in a puppy. A. Fissure consistent with open spina bifida in the entire lumbosacral region in a stillborn mongrel dog. B. Ventrodorsal plain radiographs of the vertebral column revealed a defect in the fusion of the dorsal spinous processes of the L4, L5, L6 L7 and sacral vertebrae. C and D. Dorsal view of vertebral column after maceration. Vertebral arches of C2, C7 and T1 were partially open. Opening in the lumbar and sacral vertebrae was confirmed. Reprinted with permission from Arias et al. 2008.

The defects that are associated with closed spinal dysraphism (spina bifida occulta) differ from the open form by being covered by skin with or without other intervening structures. These defects of fusion of the dorsal neural arch (which can be simple or multiple) may be asymptomatic or lead to a subcutaneous mass that may occasionally be palpated during

examination and which is composed of a meningocele and/or lipoma in dogs and cats. Common examples are sacrocaudal dysgenesis in Manx cats, dermal sinus tracts, hydromyelia and diastematomyelia (split cord) (Westworth & Sturges 2010) (Figure 10).

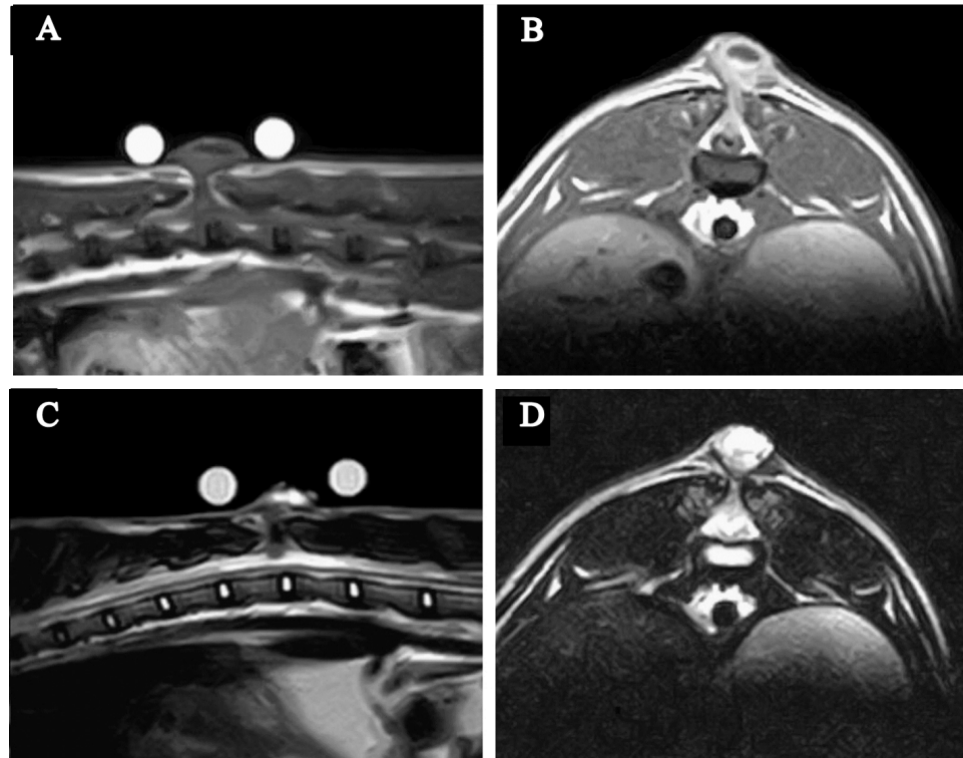


Figure 10 Cat with myelomeningocele with tethered spinal cord syndrome. Markers on the skin indicate the cranio-caudal extent of the cutaneous mass. Sagittal and transverse T1-weighted (A,B) and T2-weighted images (C,D). There is a communication between the subarachnoid space and the cutaneous mass through a defect of the dorsal lamina in a cat with myelomeningocele with tethered spinal cord syndrome. Reprinted with permission from Ricci et al. 2011.

Sacrocaudal dysgenesis is a complex form of closed spinal dysraphism, which is characterised by dysgenesis or agenesis of the coccygeal and sacral vertebrae and the associated sacral and caudal spinal cord segments, and occasionally caudal lumbar spinal cord segments. Meningoceles, subcutaneous cysts with or without cerebrospinal fluid leaking fistulas, spinal cord and cauda equina absence or shortening, central canal defects, syringomyelia, diastematomyelia, abnormal organisation of grey matter and intradural or filum terminale lipomas associated with or without tethered spinal cord have been reported

as associated anomalies (James et al. 1969; Martin 1971; Deforest & Basrur 1979; Newitt et al. 2008; Westworth & Sturges 2010).

The mutant allele known as Manx (gene symbol M) in the domestic cat has been the subject of numerous investigations. The allele is inherited as a dominant and Manx taillessness is the heterozygous expression (homozygote is a prenatal lethal) (Robinson 1993) (Figure 11).

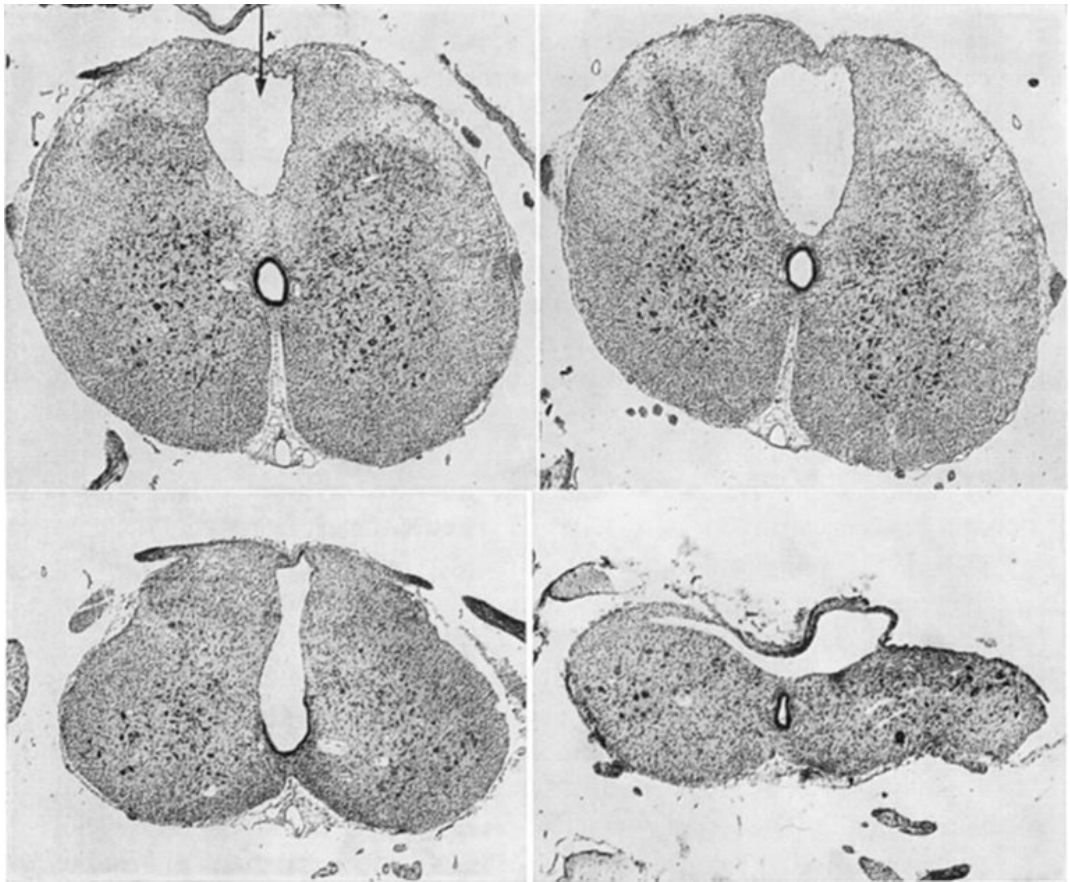


Figure 11 Cross section of the spinal cord and adjacent structures at various levels in a Manx cat: cranial lumbar area (top left) with cavity in dorsal funiculi, middle lumbar cord (top right) with enlarged cavity in dorsal funiculi, caudal lumbar cord (bottom left). The cavity is now confluent with the central canal and sacral cord (bottom right). The cord is flattened dorsoventrally. The lesion is separated from the central canal and is covered dorsally by ectoderm. Thionin stain. Reprinted with permission from Martin 1971.

1.1.2.3 Malformations originating in the embryonic period of development

The malformations originating in the embryonic period, first 34 days following fertilization of the ovum in dogs, are caused by defects in formation, and may be associated with neural tube defects (Pretzer 2008). Defects of segmentation may occur secondarily (Westworth & Sturges 2010).

Failures of formation arise as a result of the absence of a structural element of a vertebra. It can affect any part of the vertebral ring: lateral, ventral, ventrolateral, dorsal, or dorsolateral. The type of deformity depends therefore on the area of the vertebral ring affected, which will alter normal growth patterns eventually. These malformations consist of butterfly vertebrae and hemivertebrae.

Butterfly vertebrae are malformed vertebrae, which get their name from their morphological similarity to *Lepidoptera* spp on the ventrodorsal radiographic view. The sagittal cleft appearing in the vertebral body (bifid centrum formation) results from the incomplete intradiscal migration of notochordal material (Tsou et al. 1980). As a formation defect (partial or complete) affects the ventral and central portions of the vertebral body, two dorsolateral fragments of bone attached to the neural arch are left. They are often encountered asymptotically in brachycephalic screw-tailed breed dogs during unrelated diagnostic imaging investigations (Morgan 1968). This is important in the context of our research as it may lead to various degree of kyphosis, more especially if the abnormal vertebra is associated with centrum hypoplasia.

Hemivertebrae are bony remnants that abnormally developed and can be fully segmented or present as segmental defects: semisegmented or nonsegmented. Segmented hemivertebrae still have growth plates both cranially and caudally, semisegmented

hemivertebra present with fusion to a cranial or caudal vertebra and finally a nonsegmented vertebra has not separated from either the cranial or caudal vertebra. They are described as solitary, double (balanced/unbalanced) or multiple and it is believed that they result from asynchronous development of hemimetameric pairs. A unilateral absence of vascularisation is suspected for these malformations (Tsou et al. 1980) (Figure 12).

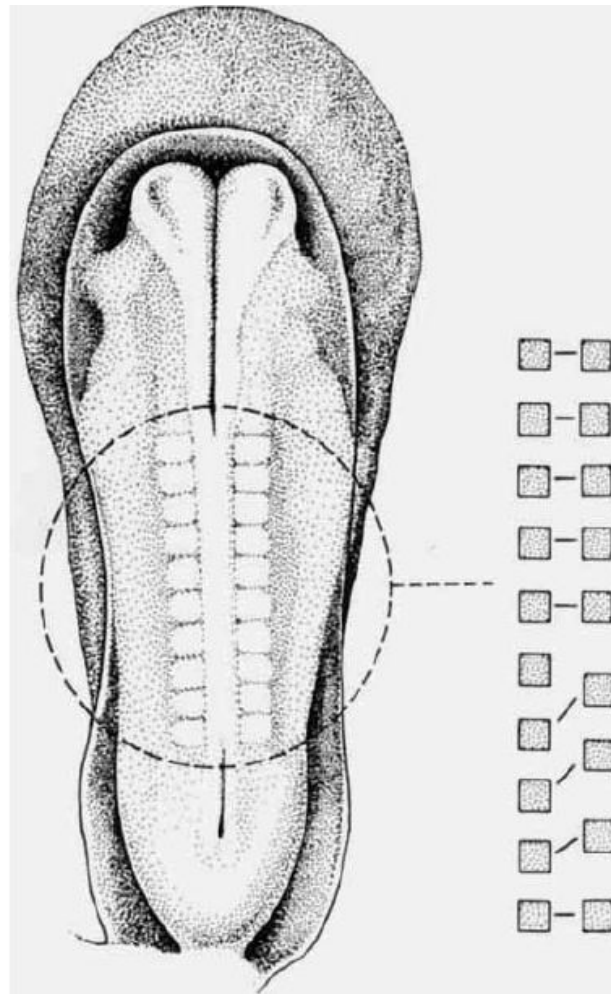


Figure 12 Schematic illustration of the pairing defect of sclerotomic cells as a result of asynchronous development of hemimetameric pair. If the paired somite derivatives are not in the same developmental phase by the time of midline fusion, the tardy side may shift one segment caudad. At the level of initial discrepancy a solitary hemivertebra develops. This is believed by the authors to be the most common mechanism of hemivertebra formation. Reprinted with permission from Tsou et al. 1980.

The term hemivertebra refers to the resulting laterally wedged vertebra. In small animals, the “classic” hemivertebra would result from a failure to form one sagittal half of the vertebra; including the centrum and the neural arch leading to the formation of a variable degree of scoliosis. Interestingly, on occasions, if a second hemivertebra contralateral to the first one occurs, the deformity is counterbalanced (double balanced hemivertebrae) (Figure 13).

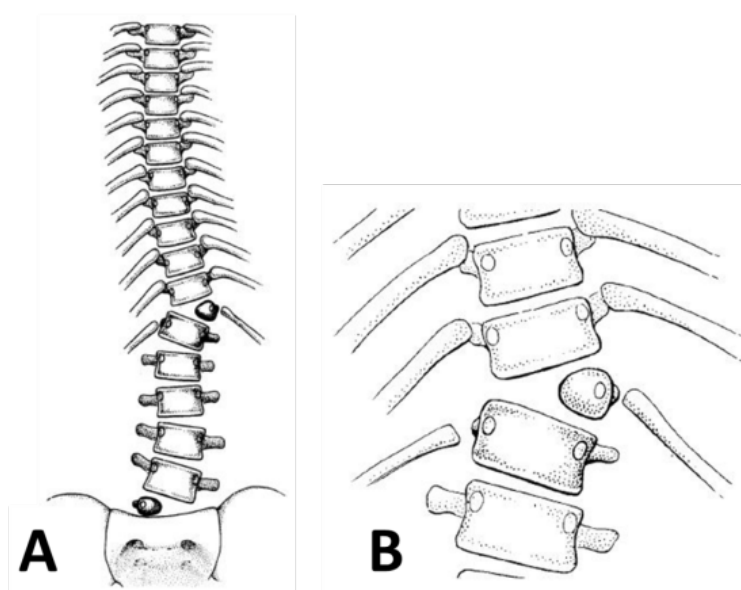


Figure 13 Hemivertebrae variations: (A) Double balanced hemivertebra. Two asynchronous pairs deployed tardy hemimetamer on contralateral sides. (B) Solitary hemivertebra as a result of asynchronous development of hemimetameric pair. Reprinted with permission from Tsou et al. 1980.

In man, other malformations of this period would include vertebral aplasia and hypoplasia secondary to hemimetamer aplasia and hypoplasia but also rib and transverse process fusions secondary to respective coalition (Tsou et al. 1980). Rib and transverse process fusion has rarely been reported in dogs (Grenn & Lindo 1969) (Figure 14).

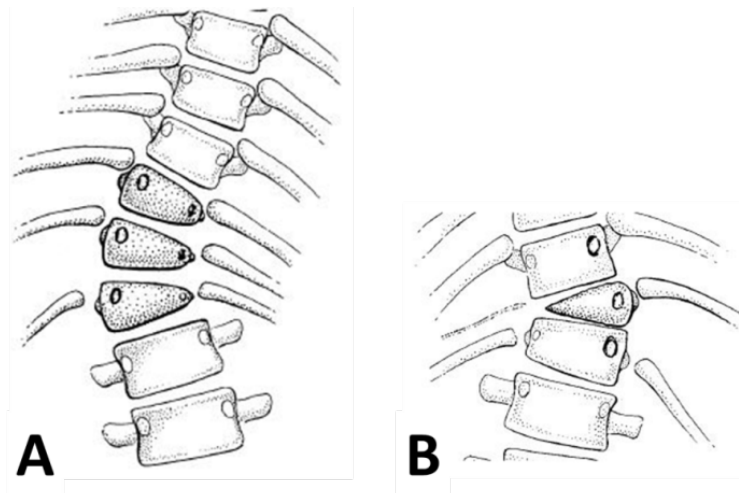


Figure 14 Hemimetamer hypoplasia and aplasia: (A) Hemimetamer hypoplasia, mild. (B) Single hemimetamer aplasia, solitary hemivertebra. The medial border of this type of hemivertebra is irregular and crosses the midline. Contralateral rib fragments may persist. Reprinted with permission from Tsou et al. 1980.

1.1.2.4 Malformations originating in the foetal period of development

Vertebral column malformations occurring in this period are secondary to defects in formation and most particularly subsequent to failure of segmentation.

During embryogenesis, segmentation of the paraxial mesoderm is the first important step in somitogenesis (somite formation). The latter involves two mechanisms which have been named the clock and waterfont model as mentioned previously. In this model, the first step, the wavefront or determination front, is associated with the elongation of the caudal end of the body (cells from the most posterior non segmented part of the primitive streak). The elongation occurs by active division of cells in this area under the influence of a high concentration of FGF-8 in comparison to more cranially, where cells are older with a lower concentration of FGF-8, broken down over time. Conversely, the cells closer to the last-formed somite become exposed to retinoic acid (RA), produced in the most caudal somites and which action opposes that of FGF. The balance of FGF and retinoic acid will

eventually allow them to enter segmentation *per se*. This is characterised by the expression of Mesp-2 (mesoderm posterior protein), which prefigures a future somite (Figure 15).

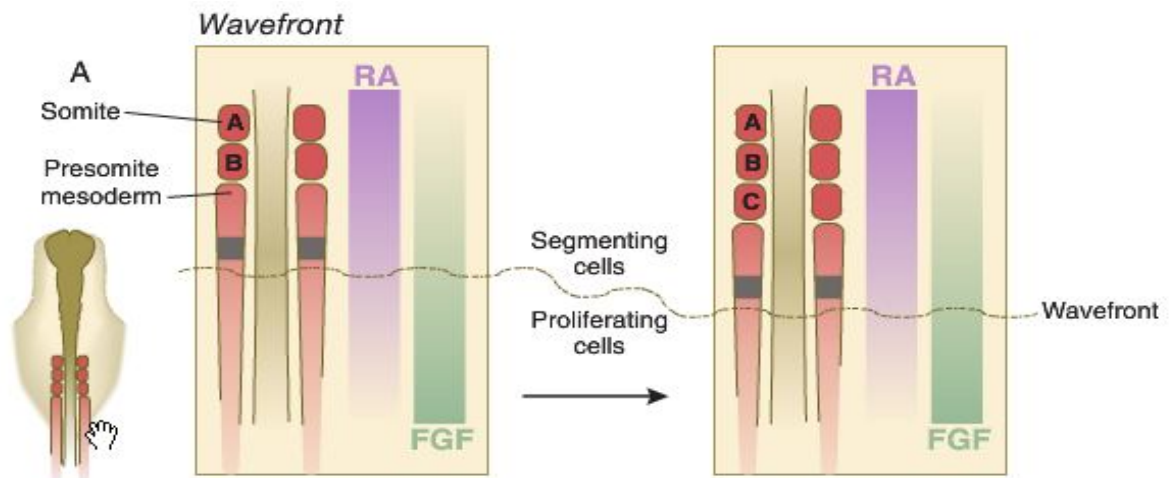


Figure 15 The wavefront: consisting of opposing gradient of retinoic acid (RA) and fibroblast growth factor-8 (FGF). Reprinted with permission from Carlson 2014.

Next, the segmentation clock is initiated in the presomitic cells that have the adequate RA/FGF gradient and expressing Mesp-2 by many molecules including Notch, Wnt, and FGF pathways. The complete mechanism of clock initiation is not completely understood. In the chick model, lunatic fringe (gene whose role is to establish the anterior boundary of somites in embryonic development) becomes concentrated at the future anterior border of the somite, and c-hairy (a homologue of a segmentation gene in *Drosophila*) becomes concentrated along the future posterior border. Also, at the anterior border of the forming somite, cells express the ephrin receptor (subfamily of receptor protein-tyrosine kinases) Eph A and at the posterior border express ephrin ligand ephrin B, the cells from the two adjacent somites are prevented from mixing and a fissure forms between the 2 somites (Figure 16) (Carlson 2014).

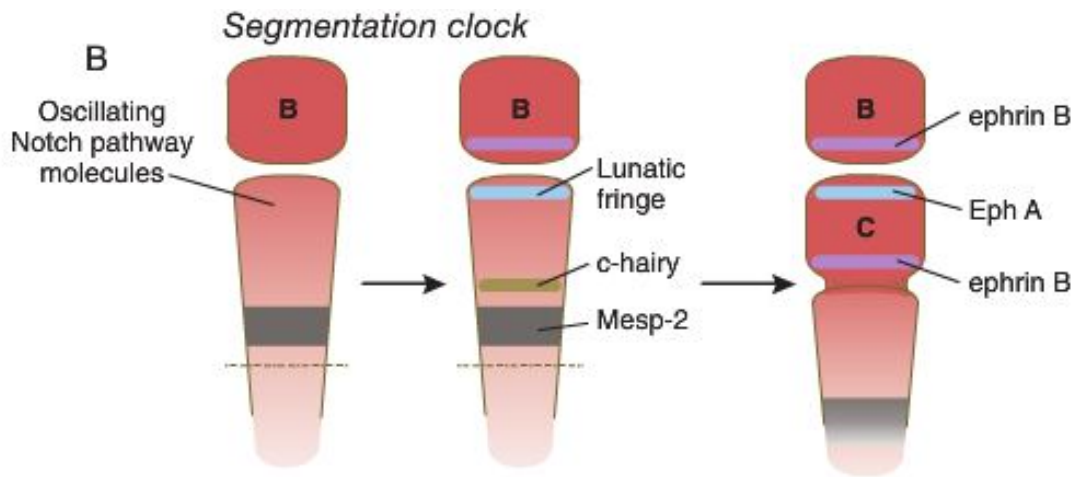


Figure 16 The segmentation clock: oscillation of molecules in the Notch pathway stimulates the expression of lunatic fringe at the anterior and c-hairy at the posterior border of a future somite. Later, interactions between Eph A and Ephrin B maintain the intersomitic space. Reprinted with permission from Carlson 2014.

Two or more vertebrae may then fail to completely separate and divide with concomitant partial or complete loss of a growth plate. It is believed that because they occur later in development, they are not so commonly associated with other defects (Tsou et al. 1980). Embryologically, segmentation defects result from two adjacent somites or their associated mesenchyme not separating properly. They are classified according to the region and the number of vertebrae affected. Block vertebrae, centrum hypoplasia or aplasia, as well as segmentation defects of the neural arch apophyseal joint and of the costovertebral joint are the congenital anomalies occurring during that period.

Block vertebrae involve the entire vertebrae, whereas defects of specific regions of the vertebral ring create unilateral bars. They can include any part(s) of the vertebrae (vertebral arch with fused non articulated processes, or centrum with or without the intervertebral disc formed). Although often clinically asymptomatic, clinical signs may occur in case of spinal cord compromise (spinal deformities, vertebral canal stenosis, and intervertebral disc disease secondary to instability, ligament hypertrophy or abnormal loading of adjacent vertebra) (Malik et al. 2009).

Anomalies of the centrum affect the development of the vertebral body, resulting in decreased longitudinal growth and subsequent deviation of the vertebral column. As the centrum development is independent of neural arch growth, the latter is usually spared. These malformations referred to as centrum aplasia and hypoplasia are caused by a defect in formation or segmentation and can be unilateral or bilateral. Although vascularisation defects or teratogenous substances have been incriminated as possible causes, their true aetiology is currently unclear. Figure 17 illustrates the various patterns of centrum defects. Screw-tailed breed dogs have been reported with such anomalies and as has the German short-haired pointer, in which the condition is inherited (autosomal recessive) (Kramer et al. 1982). Cats affected by mucopolysaccharidosis II with shorter vertebral bodies have been reported (Mazrier et al. 2003).

A summary of the congenital vertebral malformations in man is given in Figure 18. Other congenital vertebral malformations such as articular facet aplasia/dysplasia, transitional vertebrae, spinal stenosis and atlanto-axial subluxation are not discussed in this work.

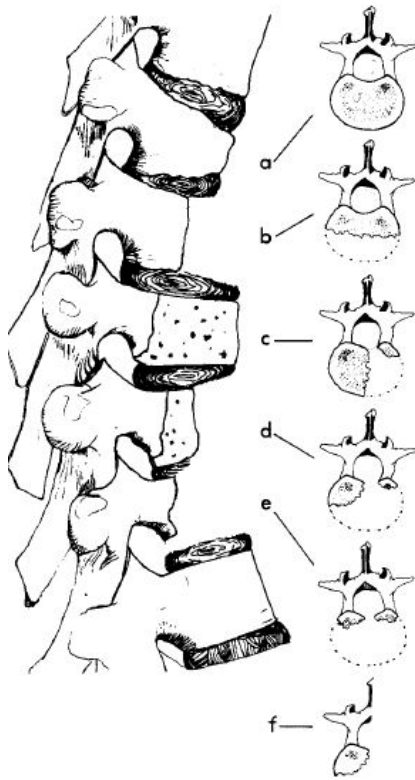


Figure 17 Centrum hypoplasia and aplasia, five common patterns seen in humans (a-e): a, wedge; b, posterior hemicentrum; c, lateral hemicentrum; d, posterior quadrant centrum; e, centrum aplasia. The posterior corner hemivertebra of Risser (f) is primarily an embryonic anomaly of asynchronous development of hemimetamer pair. The unpaired hemivertebra lateral centrum half suffers further anterior growth disturbance during the foetal period. The residue posterior quadrant centrum is accompanied by ipsilateral hemiarth in contrast to the intact neural arch of posterior quadrant centrum (d). Reprinted with permission from Tsou et al. 1980.

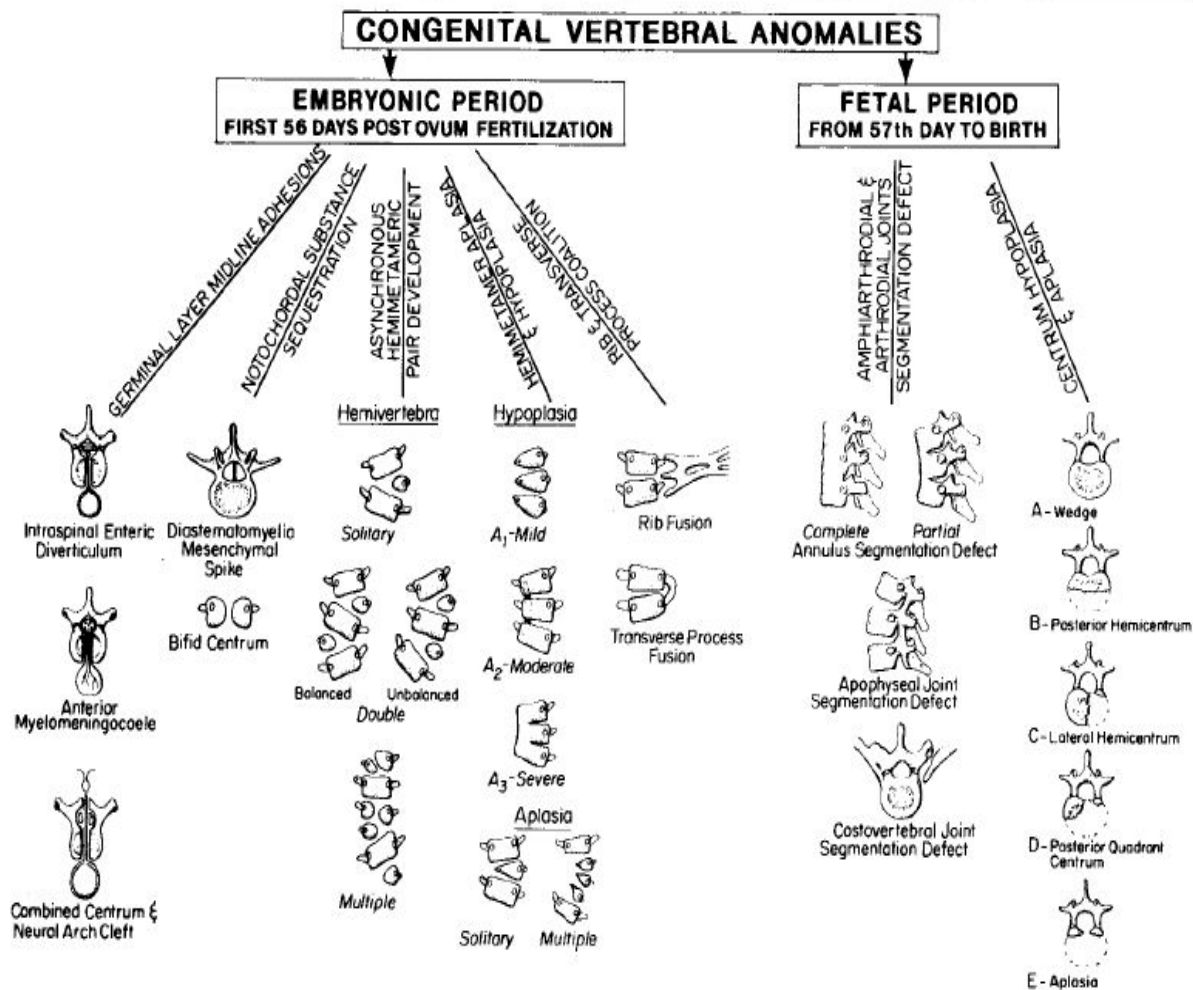


Figure 18 Schematic diagram of proposed classification of congenital vertebral anomalies in humans. All anomalies (excluding primary neural tube closure defects and occipito-C1-C2, malformations) are initially divided into two main groups, embryonic and foetal, according to the time of origin during gestation of each anomaly. Common pathogenesis guides the subsequent groupings. The specific anatomic defect is emphasized. Reprinted with permission from Tsou et al. 1980.

1.1.3 Classification systems

Classification systems and terminology need to be clear, well-defined and used consistently to ensure that a correct understanding can be made of the study of those anomalies.

In man, congenital vertebral malformations have been classified into categories on the basis of their radiographic appearance (Nasca et al. 1975; McMaster & Singh 1999; Jaskwhich et al. 2000). The first classification category includes failure of vertebral segmentation, in which portions of adjacent vertebral elements fail to divide such as block vertebra or bars. The second category consisting of failure of vertebral formation, in which a portion of a vertebral element is deficient, includes hemivertebra, wedge shape vertebra or butterfly vertebra. Based on these categories, a radiographic classification for congenital scoliosis was proposed (Nasca et al. 1975) and another for congenital kyphosis and kyphoscoliosis (McMaster & Singh 1999).

However, in veterinary medicine, congenital vertebral anomalies classification has not been clearly defined and its terminology is often not conventionally applied (Westworth & Sturges 2010). Admittedly canine malformations can be complex and inclusion in a single category is difficult but this should not deter from considering the refinement of classification schemes. In fact, only a single canine study has used the classification system of Nasca et al (1975) (Besalti et al. 2005) (**Figure 19**), and in one abstract wedging of the canine vertebral body has been classified as unilateral, dorsal, and ventral (Volta et al. 2005). The McMaster radiographic classification scheme had nonetheless not been evaluated in dogs and suggested closer attention. The latter is particularly attractive as it focuses on malformations leading to kyphosis and kyphoscoliosis, with the former being the most common vertebral column deformity in dogs (**Figure 20**) (Dewey et al. 2015).

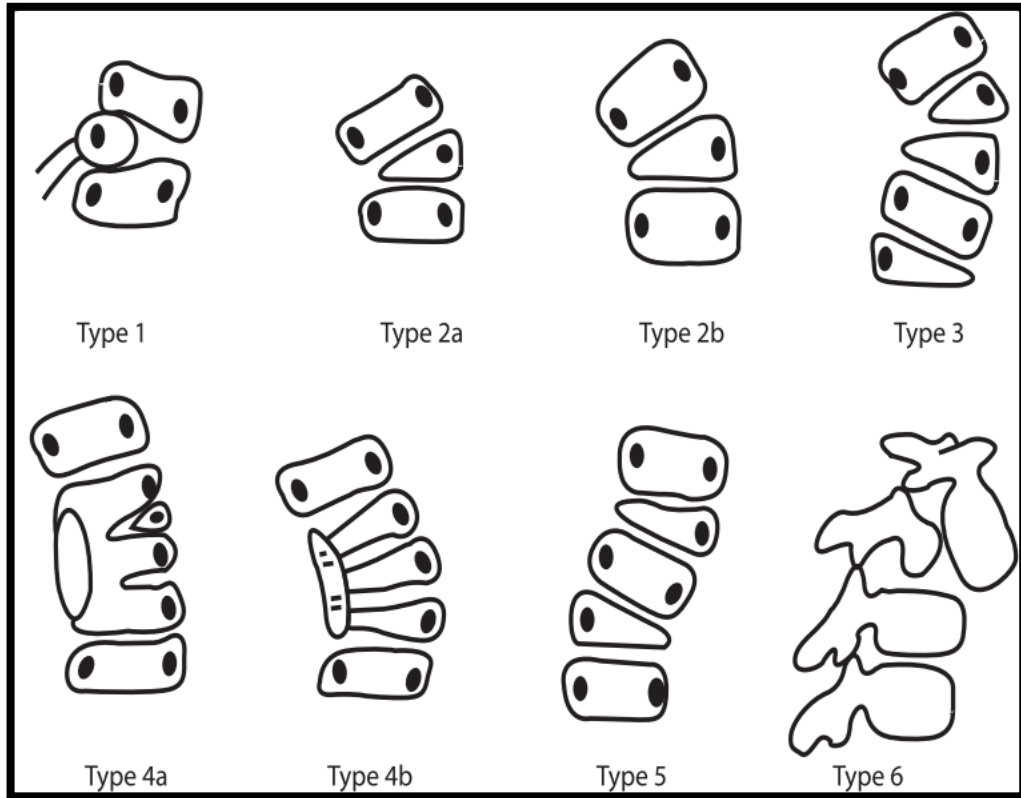


Figure 19 Classification system of Nasca et al (1975) used in veterinary medicine for five clinical cases. Reprinted with permission from Besalti et al. 2005.

DEFECTS OF VERTEBRAL-BODY SEGMENTATION	DEFECTS OF VERTEBRAL-BODY FORMATION		MIXED ANOMALIES
<p>Partial</p> <p>ANTERIOR UNSEGMENTED BAR</p>	<p>Anterior and Unilateral Aplasia</p> <p>POSTEROLATERAL QUADRANT VERTEBRA</p>	<p>Anterior and Median Aplasia</p> <p>BUTTERFLY VERTEBRA</p>	<p>ANTEROLATERAL BAR AND CONTRALATERAL QUADRANT VERTEBRA</p>
<p>Complete</p> <p>BLOCK VERTEBRA</p>	<p>Anterior Aplasia</p> <p>POSTERIOR HEMIVERTEBRA</p>	<p>Anterior Hypoplasia</p> <p>WEDGED VERTEBRA</p>	

Figure 20 McMaster classification for vertebral anomalies. Drawings showing the different types of vertebral anomalies that produce a congenital kyphosis or kyphoscoliosis. Reprinted with permission from McMaster & Singh 1999.

1.2 Deviations of the vertebral column, methods of evaluation and clinical implication

1.2.1 *Deviations of the vertebral column*

Three planes exist in which deviations of the vertebral column may occur. They are termed kyphosis, scoliosis and lordosis and are respectively deviations in the dorsal, lateral and ventral planes (Kealy et al. 2011).

As previously mentioned, congenital vertebral malformations causing secondary kyphosis and scoliosis are relatively common in dogs, especially in the brachycephalic so called “screw-tailed” breeds such as English bulldogs, French bulldogs, Boston terriers and Pugs. Patients suffering from these abnormal spinal curvatures are often asymptomatic with malformations uncovered as incidental findings during unrelated radiography studies. The clinical signs that may be observed in affected patients are usually those of a progressive compressive myelopathy secondary to vertebral canal stenosis but also to instability of the vertebral column related to the degree of spinal curvature (Westworth & Sturges 2010; Moissonnier et al. 2011; Aikawa et al. 2014).

The plane of the deformity is important. In humans and dogs, the vertebral malformations that tend to cause neurological deficits are primarily those that lead to kyphosis of the vertebral column (Dewey et al. 2016).

Diagnostic imaging allows diagnosis and characterization of congenital vertebral malformations in dogs. Radiography, myelography, computed tomography (CT) and magnetic resonance imaging (MRI) are the available modalities. Although radiography allows identification of the vertebral bony malformation, it does not give any information regarding the integrity of the spinal cord. Although myelography may address this

limitation to some extent by identifying spinal compression, it does not provide any information on the possible concurrent parenchymal lesions (eg, syringomyelia, arachnoid diverticula). Nowadays it is nowadays possible with CT and MRI to have a much more refined understanding of these malformations and their relationship with the rest of the vertebral column. CT will provide valuable information on the three-dimensional (3D) bony organization of the vertebral column in space. Multiplanar reconstruction and 3-D volume reconstruction permit intimate assessment of these malformations and secondary deformities (**Figure 21**). MRI will finally give high quality details on the spinal cord parenchyma, which may be affected in the context of those deformities (**Figure 22**).

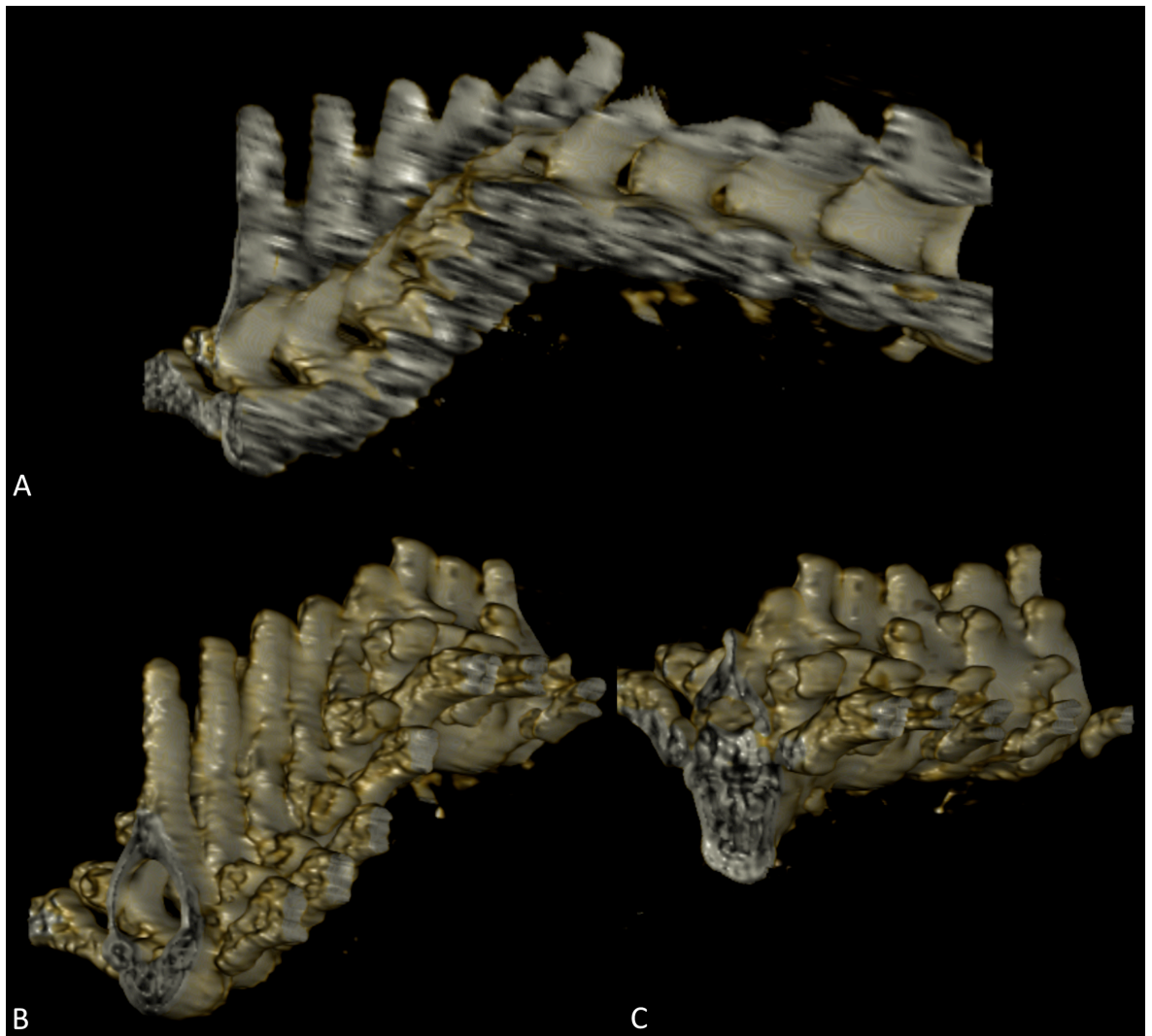


Figure 21 Reconstructed sagittal CT of a dog with a thoracic vertebral malformation. Mid-sagittal plane (A) and transverse plane at T5 (B) and T9 (C) highlighting the progressive narrowing of the vertebral canal.

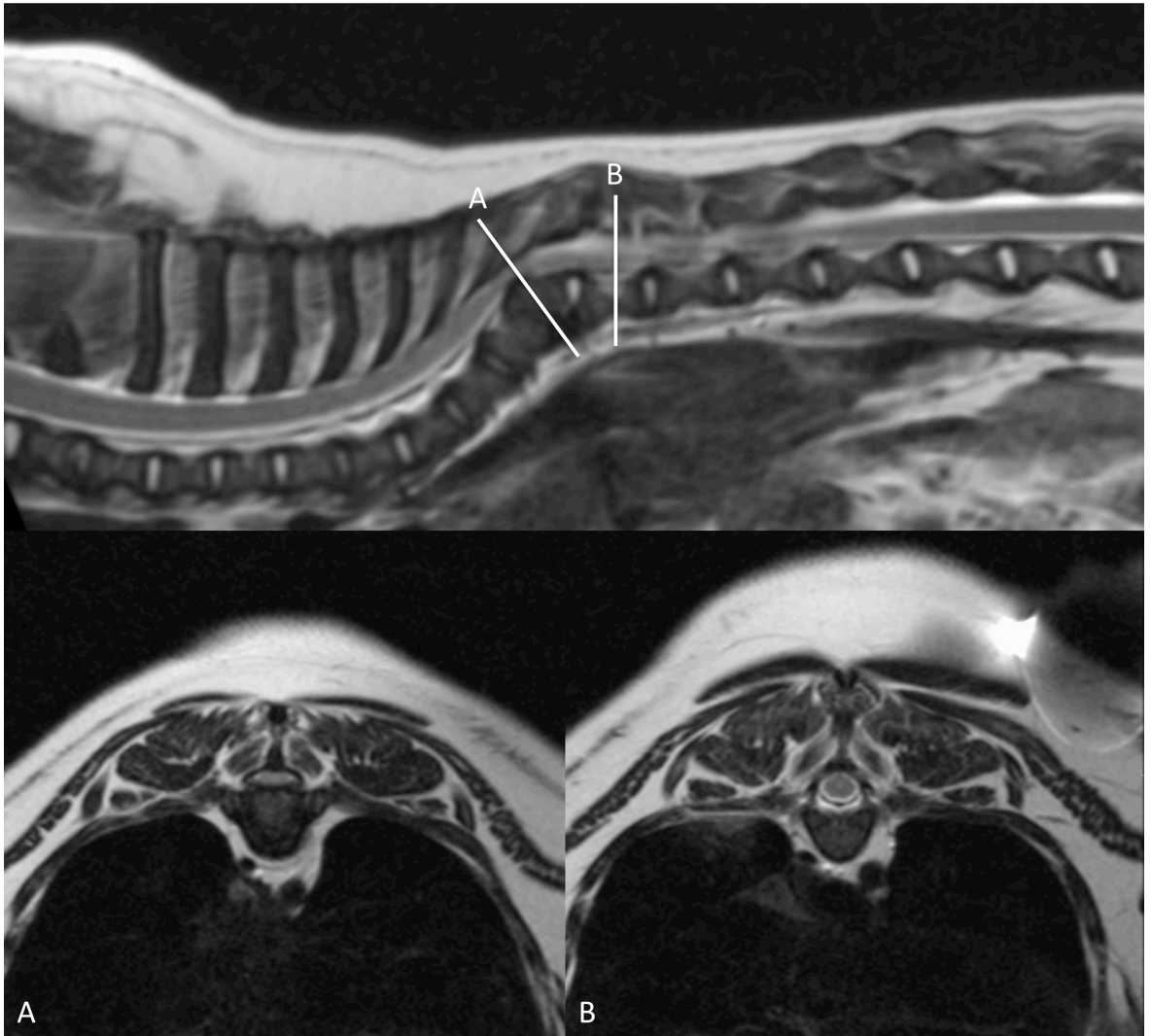


Figure 22 Sagittal T2 weighted MRI of the thoracic spine showing a T9 vertebral malformation and secondary kyphosis. Transverse T2 weighted MRI at the level of (A) and caudal to (B) the vertebral malformation highlighting the spinal cord compression.

1.2.2 Methods of evaluation of the curvature deformity

An important factor evaluated in human patients suffering from congenital vertebral malformations and causing kyphosis or scoliosis is the degree of curvature of the vertebral column. The angular magnitude of a deformity is usually quantified using radiographic techniques with the calculation of the Cobb angle (Cobb 1948). This radiographic method is widely used to guide decisions regarding progression, physiotherapy, orthotic options and surgical interventions (Nasca et al. 1975; McMaster & Singh 1999; Langensiepen et al.

2013). Various techniques have been used and assessed to calculate the Cobb angle. They include manual, digital computer-assisted (semi-automatic), automatic and even smartphone procedures (Srinivasalu et al. 2008; Tanure et al. 2010; Zhang et al. 2010; Qiao et al. 2012; Langensiepen et al. 2013). However, despite its widespread use, studies on the reproducibility of the measurements have shown variability in its intra- and inter-observer agreement (Morrissy et al. 1990; Polly et al. 1996).

The Cobb angle was originally described in 1948 for the assessment of coronal plane deformity in human patients with scoliosis. This technique consists of manual measurement of the angle on radiographs and is considered to be the gold standard. It has been adapted and used for the measurement of sagittal alignment also. Indeed, it was shown to be a reliable and reproducible method for the assessment of normal lumbar lordosis and post-traumatic kyphosis (Polly et al. 1996; Kuklo et al. 2001). In man a modified Cobb angle has been defined, for the management of post traumatic kyphosis, as the angle formed between a line drawn parallel to the superior endplate of one vertebra above the fracture and a line drawn parallel to the inferior endplate of the vertebra one level below the fracture (Keynan et al. 2006).

In the context of congenital vertebral malformation in canine patients, the Cobb angle has been used, but the technique has never been evaluated. Therefore, validating a reliable method of establishing the Cobb angle is the foundation to its adoption as a universal technique. Undoubtedly, it will help not only towards the assessment of the severity of the deformity and the monitoring of progression but it may also prove to have value in prognostication and treatment recommendations in patients that are affected neurologically.

1.2.3 Clinical implication

The fact that the congenital malformations are common incidental findings, with no associated clinical signs, most likely resides in the mild to moderate curvatures that occur. In canine patients, the degree of kyphosis secondary the vertebral malformation is related to the likelihood of developing neurological dysfunction. Scoliosis, on the other hand, does not seem to have such an important impact on the neurological status (Westworth & Sturges 2010; Dewey et al. 2015). Surgical decompression or an attempt to correct the misalignment of the spinal curvature has been reported to be successful in dogs with predominantly thoracic kyphotic deformities (Aikawa et al. 2007; Jeffery et al. 2007; Dewey et al. 2015).

Clinical signs of neurologic dysfunction in patients with thoracic vertebral malformations are consistent with the location of the malformation and thereby result in a T3-L3 myelopathy. A progressive, waxing and waning, ambulatory paraparesis with pelvic limb ataxia is often observed, and decompensation with an acute clinical deterioration may be seen. Some patients may present with an acute onset of non-ambulatory paraparesis, others may solely display hyperaesthesia in the area overlaying the spinal deformity (Dewey et al. 2015).

People with kyphotic deformities more frequently also display neurological deficits secondary to the spinal cord compression when compared to those with scoliosis. Early intervention is usually recommended in order to prevent clinical deterioration. The angular deformity is evaluated using the Cobb angle method and the surgical technique is selected based on the value of the angle: dorsal arthrodesis of the facets if the deformity is inferior to 50 degrees and anterior release technique and posterior arthrodesis if superior to 50 degrees (McMaster & Singh 2001). Other described techniques have been predicated on

the complexity of the deformation (Winter 1997). Recommendations for surgical intervention are therefore not only based on clinical presentation but also on the degree of curvature identified on radiography. The latter has never been assessed in dogs.

In dogs, there are few published reports on the surgical management of this complex disorder (Aikawa et al. 2007; Jeffery et al. 2007; Charalambous et al. 2014; Dewey et al. 2015). The abnormal vertebra is believed to lead to some instability of the vertebral segment and therefore stabilisation is recommended (Dewey et al. 2015). The two main methods are segmental spinal stabilisation (referred to as “spinal stapling”) and stabilisation with pins and polymethylmethacrylate. To relieve the spinal cord impingement caused by the malformed vertebra, a decompressive procedure (dorsal laminectomy, hemilaminectomy) performed at the same time as stabilisation has also been advocated by the same authors. Recommendation for surgical intervention is usually made on the basis of the severity and/or progression of the neurological deficit. As mentioned above, the usefulness of the degree of curvature to make a surgical decision is unknown. It is also unclear how kyphosis progresses in dogs and if surgery may have a preventative role to play in young non-affected screw-tailed breeds with congenital vertebral malformations.

1.3 Hypotheses and aims

The first aim of this study is to study the signalment and the neurological statuses of a population of screw-tailed dog breeds presenting with congenital vertebral malformations. We hypothesise that within the screw-tailed dog breeds group, congenital vertebral malformations would lead to neurological deficits in a more specific breed such as the Pug.

The second aim is to determine whether the radiographic classification scheme which had been developed for use in human (McMaster classification)(McMaster & Singh 1999) can be translated and applied to malformations of the vertebral column in brachycephalic “screw-tailed” dog breeds. The hypothesis is that the human McMaster classification method could be translated successfully to dogs with congenital vertebral malformations.

The third aim is to study the relationship between the vertebral malformations (appropriately termed based on the translated classification) and the neurological status. We hypothesise that some vertebral malformations leading to more severe kyphosis were more likely to be identified in dogs with neurological deficits.

The fourth aim is to determine whether a Cobb angle measurement technique which had been developed for use in human (Osirix software) can be translated and applied to dogs with kyphosis and kyphoscoliosis with adequate reliability. The hypothesis is that the human Cobb angle measurement technique described above can be translated and applied to spinal deformities in dogs with adequate reliability.

The fifth aim is to determine whether a relationship exist between the degree of spinal deformity (using the validated Cobb angle measurement technique) and the neurological

status of screw-tailed dog breeds. We hypothesised that dogs with more severe kyphosis would be identified in the group of dogs presenting neurological deficits.

Finally, if successful, the translated classification system of vertebral malformations and Cobb angle measurement technique could be proposed for use in veterinary medicine. The former would allow to overcome the previously discussed lack of clarity, and misuse of the terminology with these disorders and the latter allow reliable measurement of canine spinal deformities with a validated technique.

CHAPTER II MATERIAL AND METHODS

2.1 Population and neurological status

The medical records of the University of Glasgow Small Animal Hospital were retrospectively reviewed for the period September 2009 to April 2013 to identify “screw-tailed” dogs (French bulldogs, English bulldogs, Boston terriers, and Pugs). This was achieved by using the online Electronic Patient Record (EPR) research tool (Excelicare, Axys Ltd). The inclusion criteria included having had a well-positioned lateral and ventro-dorsal digital radiographs of the thoracic vertebral column, with at least a single vertebral congenital malformation present. The breed, age and sex were recorded.

If the patient was reported to have any neurological deficits associated with the vertebral malformation, the duration of clinical signs and the neurological grade at the time of presentation were then recorded. For the latter, the conventionally applied neurological grading system (0-5) was used (Sharp & Wheeler 2005). The patients were then divided into two groups, one with neurological deficits localized to the thoracic spinal cord segments (Group 1) and one without neurological deficits (Group 2). The breed, age and sex were also recorded. Statistical tests were selected by a statistician for both studies. Data was analysed using a statistical software (Minitab 16 Statistical software, Minitab Inc, State College, PA, USA). Descriptive statistics were reported as mean, range and standard deviation (SD).

2.2 Identification and classification of the congenital vertebral malformations

Radiographs for each dog were retrieved and displayed using an open-source PACS Workstation DICOM viewer software (Osirix Imaging Software, v 3.9.2, Pixmeo, Geneva, Switzerland). Two observers, blinded to the groups, recorded the number and the vertebral

level for each vertebral malformation and for each patient. Then, by consensus between them, they classified each vertebral malformation according to the system of McMaster (Figure 20, page 38), which had been translated into the classification system illustrated in Figure 23.

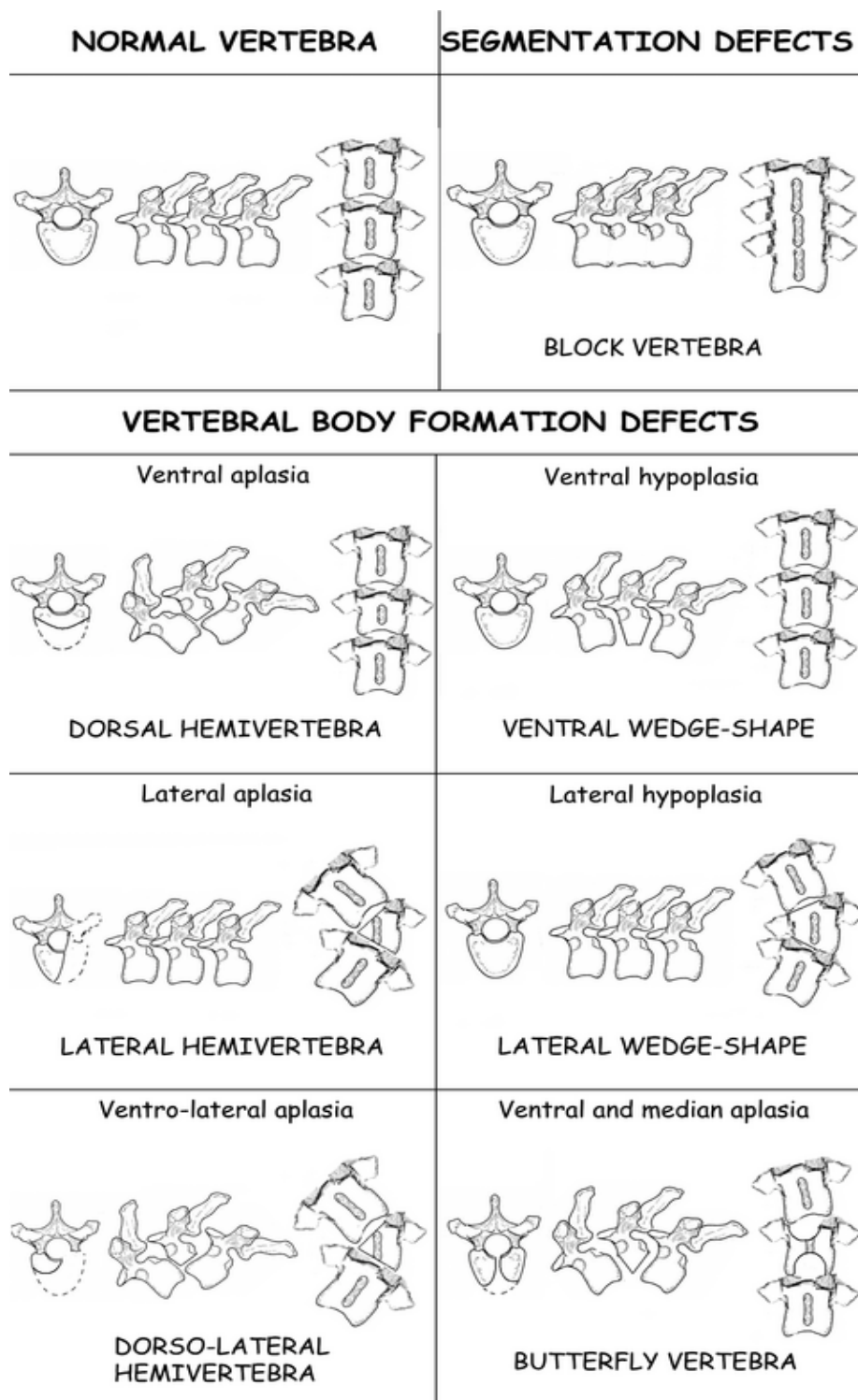


Figure 23 Schematic line drawing showing the radiographic appearance of the vertebral malformation classification system used in this study. Reprinted with permission from Gutierrez-Quintana et al. 2014.

The vertebral malformations were classified as defects of segmentation if adjacent vertebral elements had failed to divide (block vertebrae) or defects of formation if a portion of the vertebra was deficient. Defects of formation were then subclassified into ventral aplasia of the vertebral body (dorsal hemivertebra), lateral aplasia of the vertebral body (lateral hemivertebra), ventro-lateral aplasia of the vertebral body (dorso-lateral hemivertebra), ventral and median aplasia of the vertebral body (butterfly vertebra), ventral hypoplasia of the vertebral body (ventral wedge shape vertebra), and lateral hypoplasia of the vertebral body (lateral wedge shape vertebra). Figure 24 and Figure 25 illustrate the method. The presence of any other vertebral malformations, including thoracic and cervical transitional vertebrae, spina bifida and any other types, were also recorded. We were able to classify 50 of these vertebral malformations using the proposed classification system.

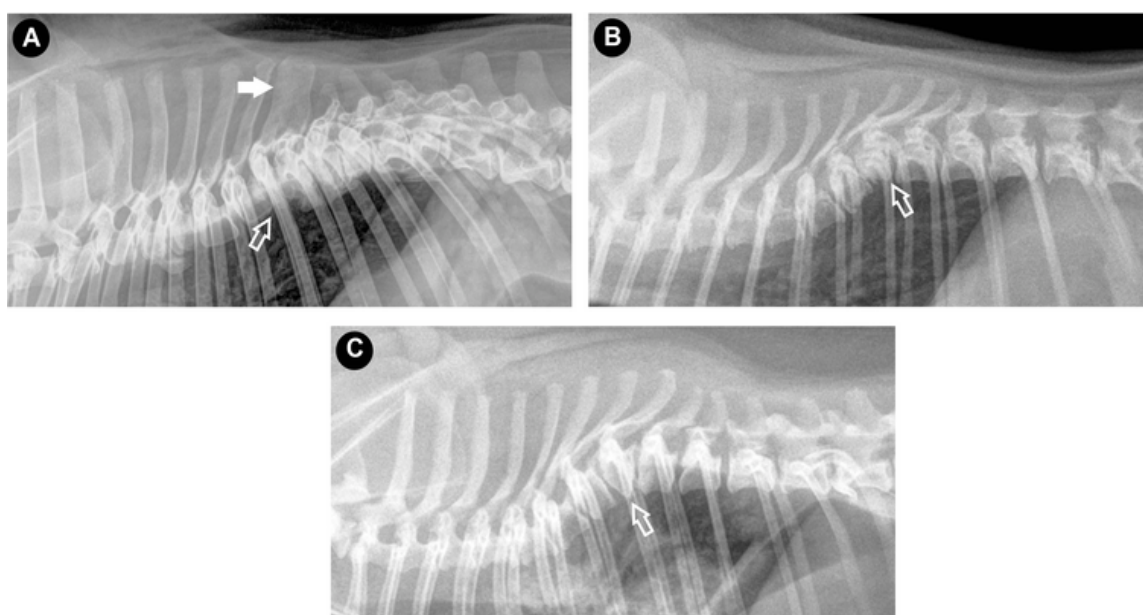


Figure 24 Congenital vertebral malformations identified on lateral radiographs of the thoracic vertebral column. (A) Block vertebrae, where there is failure of normal segmentation of the vertebrae, evident as the failure of division of T8 and T9 vertebral bodies (open arrow) and spinous process (solid arrow). (B) Ventral hypoplasia of T8 vertebral body (ventral wedge shape vertebra) (arrow) with kyphosis. (C) Ventral aplasia of T8 vertebral body (dorsal hemivertebra) (arrow) with more severe kyphosis. Reprinted with permission from Gutierrez-Quintana et al. 2014.

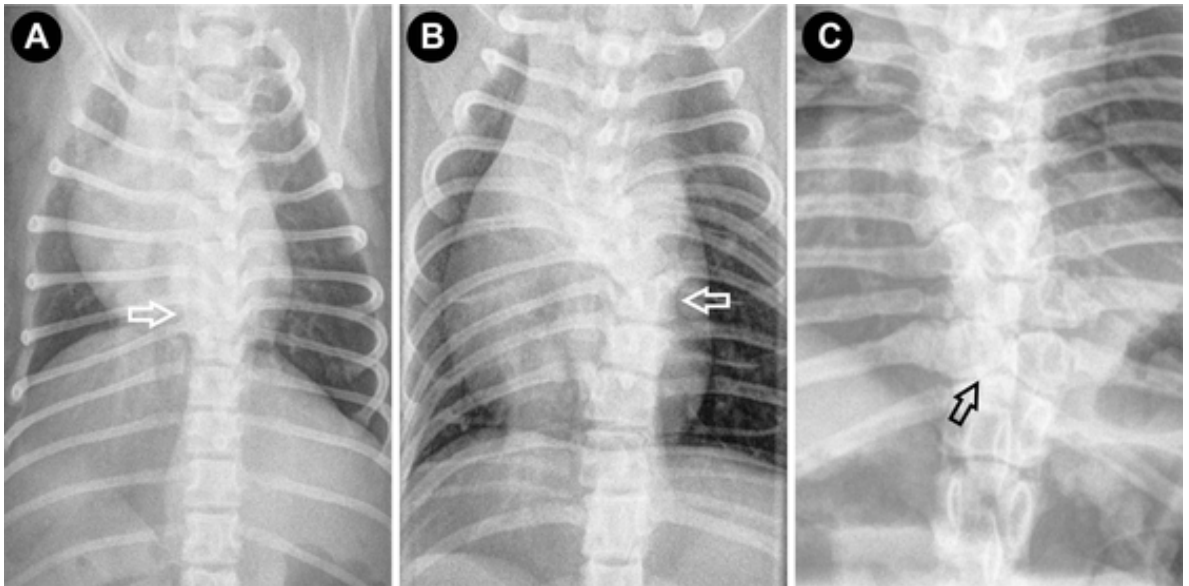


Figure 25 Congenital vertebral malformations identified on ventro-dorsal radiographs of the thoracic vertebral column. (A) Ventral hypoplasia of T8 vertebral body (arrow, this is the same case as figure 2B): no evidence of scoliosis is evident on the ventro-dorsal view if there is no lateral hypoplasia. (B) Ventro-lateral aplasia of T8 vertebral body (dorso-lateral hemivertebra) (arrow). This case had similar changes to figure 2C on the lateral view. (C) Ventral and median aplasia of the vertebral body (Butterfly vertebra) (arrow). Reprinted with permission from Gutierrez-Quintana et al. 2014.

2.3 Congenital thoracic vertebral malformations and neurological status

The data corresponding to the type of congenital thoracic vertebral malformations and neurological status obtained in the results of the two previous sections were reviewed.

Using the aforementioned statistical software, a Fisher exact test was used to compare the number of vertebral malformations between the two groups of dogs, with significance defined as $P < 0.05$. For that the number of dogs with severe vertebral malformations (ventral aplasia of the vertebral body, lateral aplasia of the vertebral body, and ventro-lateral aplasia of the vertebral body) and with less severe vertebral malformations (ventral and median aplasia of the vertebral body, ventral hypoplasia of the vertebral body and other unclassified vertebral malformations) in each of the groups was calculated.

2.4 Cobb angle measurement method assessment

Three observers evaluated independently the radiographs using the open-source PACS Workstation DICOM viewer software mentioned above (section 2.2, page 48). The data set was assessed twice by the 3 observers which included two board certified veterinary neurologists and a first year veterinary neurology resident that were blinded to the dog groups. Data set had not been randomised; the second assessment was done several weeks apart from the first one. The degree of spinal curvature was assessed on the ventro-dorsal view for scoliosis and on the lateral view for kyphosis. The software included a plugin that allows for the Cobb angle to be calculated automatically. To do so, once the plugins had been selected, a reference line was traced and superposed to the cranial vertebral end plate of the first vertebra cranial to the malformed vertebra and the same was done for a second line, parallel to the caudal vertebral end plate of the first caudal vertebra. The Cobb angle was then automatically calculated by the software and displayed on the screen (Figure 26). If multiple malformations were present, each was evaluated individually unless they were adjacent, in which case the most significant vertebral malformation was selected, based on a consensus of the observers.

In order to analyse the measurement reliability of the technique described above, the intraclass correlation coefficient (ICC) two-way mixed model on absolute agreement was used and it was calculated for both intra-rater and inter-rater reliability. The value of the ICC can range from 0 to 1, with a higher value indicating better reliability. ICC less than 0.40 was considered as poor; 0.40 to 0.59 as fair; 0.60 to 0.74 as good, and 0.75 to 1.00 as excellent. This refers to previously published data (Shrout & Fleiss 1979; Fleiss 1986).

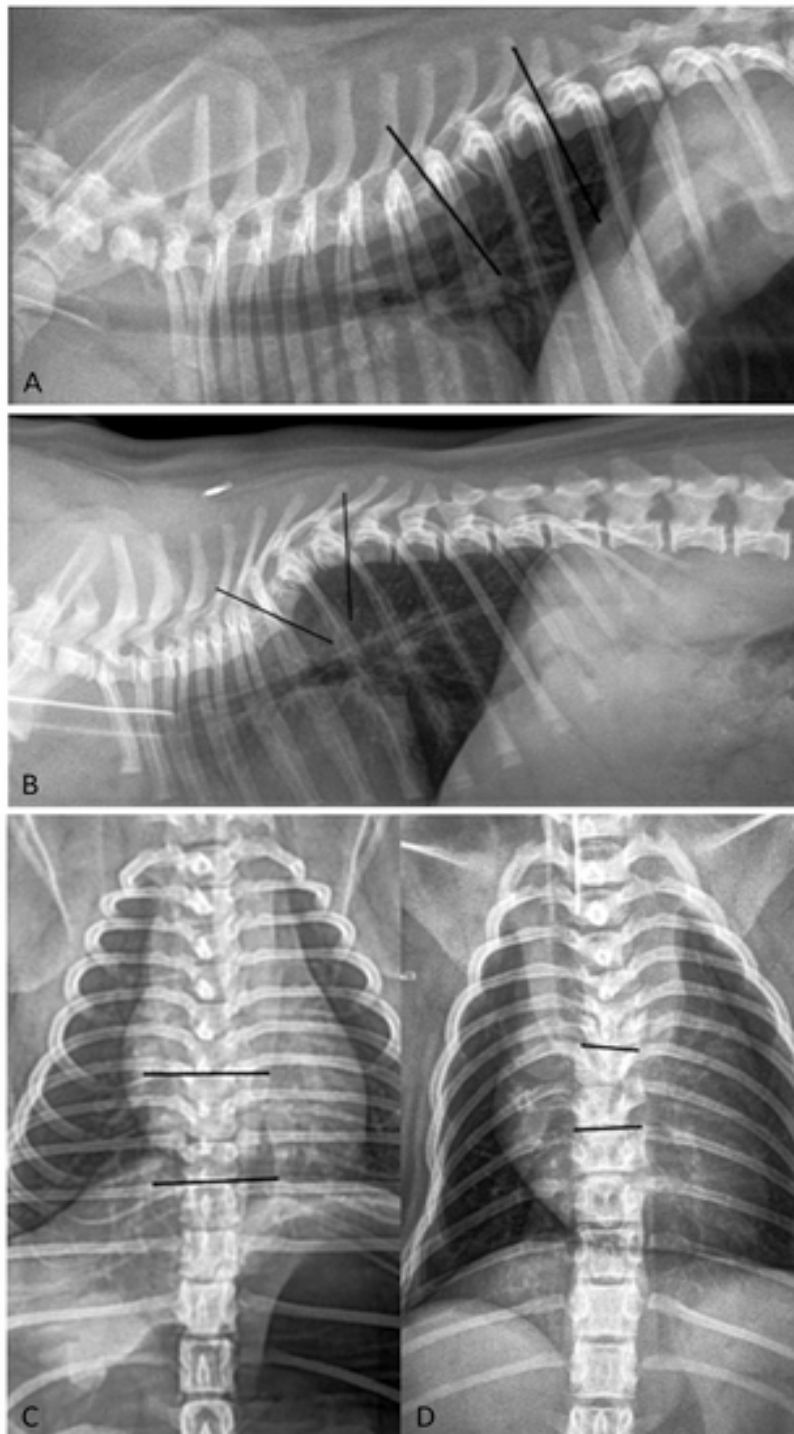


Figure 26 Cobb angles measurements. Lateral and ventro-dorsal radiographs of a neurologically normal Pug with a congenital vertebral malformation at the eighth thoracic vertebra (T8) identified as an incidental finding (A,C) and a clinically affected Pug with a related congenital vertebral malformation at the seventh thoracic vertebra (T7) (B,D). The placement of the reference lines for the calculation of the kyphotic (lateral radiograph) and scoliotic (ventro-dorsal radiograph) angles is shown. The lines pass over the cranial vertebral end plate of T7 and over the caudal vertebral end plate of the ninth thoracic vertebra (T9) in the normal Pug (A,C); and similarly over the vertebral end plates of the sixth thoracic vertebra (T6) and T8 in the affected Pug (B,D). Reprinted with permission from Guevar et al. 2014.

2.5 Cobb angles, spinal deformity and neurological status

The data set corresponding to the Cobb angles of spinal deviation for scoliosis and kyphosis was then reviewed and compared with the data collected on neurological status (section 2.1, p48).

Data was analysed using statistical software (Minitab 16, Minitab Inc, Coventry, UK and SPSS 21, IBM Corp, Chicago, IL, USA). Descriptive statistics were reported as mean, median, range and standard deviation (SD). The Mann-Whitney test was used to compare both groups as the data was not normally distributed. Statistical significance was set for $P < 0.05$. When statistics were calculated to compare the two groups, only one set of values from one observer was used (as the ICC values were excellent). When multiple vertebral malformations were present the one with the highest kyphotic and/or scoliotic angle was used for the comparison between groups.

CHAPTER III RESULTS

3.1 Population and Neurological Status

The patients included in this study are summarised in Table 2 (page 57).

Twenty-eight dogs were included and the breed population consisted of eleven Pugs, eleven English bulldogs, three French bulldogs, and three Boston terriers. The mean age was 2.5 years (range: 4 months-14 years, SD: 2.86 years). There were twenty males including two neutered and eight females of which only one was neutered.

Twelve dogs were neurologically affected (Group 1) and 16 dogs did not exhibit neurological deficits (Group 2) at the time of thoracic spinal radiography. The 12 dogs with the neurological deficits included nine Pugs, two English bulldogs and one French bulldog. The mean age was 2.4 years (range: 4 months-7.5 years, SD: 2.4 years). There were six males (one neutered) and six females (one neutered).

The mean duration of neurological deficits prior to presentation was 68 days (range: 1–240 days, SD: 69 days). Ambulatory paraparesis and ataxia (grade 2) was reported in nine dogs, nonambulatory paraparesis (grade 3) was observed in two dogs and one was paraplegic with presence of nociception (grade 4).

All dogs within Group 1 were identified to have had MRI of the thoracic spine using the same 1.5 Tesla scanner (Magnetom Essenza, Siemens, Camberley, United Kingdom). The MRI sequences that were acquired for all those patients consisted of sagittal T2-weighted images and transverse T2-weighted and T1-weighted images. Spinal cord compression was identified in all of the affected dogs. MRI confirmed that the congenital vertebral malformation was directly responsible for the spinal cord compression in ten of the dogs,

and no other abnormalities could be identified. One dog had an intervertebral disc herniation at the level of the intervertebral disc adjacent to the vertebral malformation. Finally, another dog was diagnosed with discospondylitis and secondary empyema in the intervertebral disc adjacent to the vertebral malformation.

The 16 dogs with no neurological deficits (Group 2) included nine English bulldogs, three Boston terriers, two Pugs, and two French bulldogs. The mean age was 2.6 years (range: 7months-14 years, SD: 3.2 years). There were 14 males (one neutered) and two females. None of the Group 2 dogs had MRI of the thoracic spine. (Table 2, 3)

<i>Variables</i>	<i>Group1</i>	<i>Group2</i>	<i>Total population</i>
Population	12 (0.43%)	16 (57%)	28 (100%)
Breed	Pug: 9 (75%) EB: 2 (17%) FB: 1 (8%) BT: 0	Pug: 2 (12.5%) EB: 9 (56%) FB: 2 (12.5%) BT: 3 (19%)	Pug: 11 (39%) EB: 11 (39%) FB: 3 (10.5%) BT: 3 (10.5%)
Sex	Female: 6 (50%) Male: 6 (50%)	Female: 2 (12.5%) Male: 14 (87.5%)	Female: 8 (28%) Male: 20 (72%)
Age	Mean: 2.4 y Range: 4m-7.5y SD: 2.4	Mean: 2.6 y Range: 7m-14y SD: 3.2	Mean: 2.5 y Range: 4m-14y SD: 2.8

Table 2 Incidence, breed, sex and age of the population. EB: English bulldog, FB: French bulldog, BT: Boston terrier and SD: Standard deviation. Reprinted with permission from Guevar et al. 2014.

<i>Grade</i>	<i>Clinical signs</i>	<i>Group1</i>	<i>Group2</i>
0	Normal		16/28 (57%)
1	Spinal pain	0/12 (0%)	
2	Ambulatory paraparesis	9/12 (75%)	
3	Non-ambulatory paraparesis	2/12 (17%)	
4	Paraplegia with intact deep pain perception	1/12 (8%)	
5	Paraplegia with absent deep pain perception	0/12 (0%)	

Table 3 Clinical 0 to 5 grading scale for thoracolumbar spinal cord lesions (Sharp & Wheeler 2005) and incidence in the two groups. Reprinted with permission from Guevar et al. 2014.

3.2 Identification and classification of the congenital thoracic vertebral malformations

A total of 362 vertebrae were evaluated, as two of the dogs had 12 thoracic vertebrae ((26 x13 thoracic vertebrae) + (2x12 thoracic vertebrae) = 362). A congenital malformation was identified in 85 (n= 85/362; 23.5%) vertebrae. Eighteen (n=18/28; 64.2%) of the dogs were diagnosed with multiple malformations (more than one malformation).

The vertebra most commonly malformed was T7 (11 dogs), followed by T8 (eight dogs) and T12 (eight dogs). Figure 27 summarises the types and number of malformation observed along the thoracic vertebral column.

Of the 35 vertebral malformations that failed to meet the criteria for classification, 26 had a shorter vertebral body length with a normal shape, four had fused spinous processes with normal vertebral bodies, three were transitional vertebrae and two were diagnosed with spina bifida.

Of the 50 vertebral malformations classified, only one was a defect of vertebral segmentation and the remainder 49 were defects of vertebral formation. The malformation most commonly identified was the butterfly vertebra, seen in 24 vertebrae (n=24/362; 6.6%), followed by the ventral wedge shape vertebra in 20 vertebrae (n=20/362; 5.5%), the dorsal hemivertebra in three vertebrae (n=3/362; 0.8%), the dorso-lateral hemivertebra in two vertebrae (n=2/362; 0.5%) and the block vertebra in one vertebra (n=1/362; 0.3%). No lateral hemivertebra or lateral wedge shape vertebra were identified in this study. The data is summarised in the first 2 columns of Table 4.

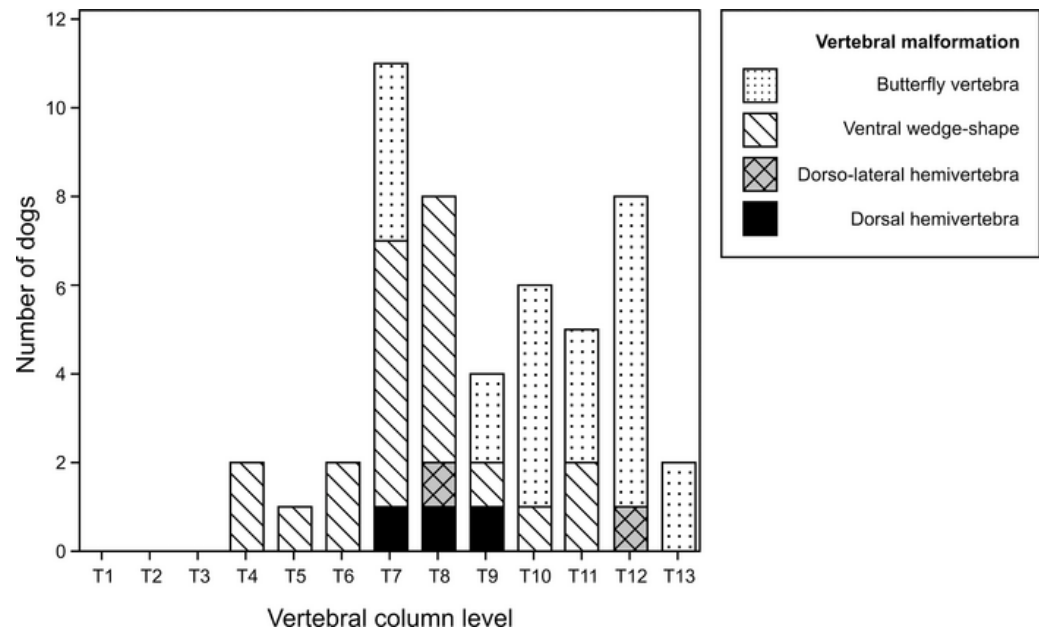


Figure 27 Histogram showing the frequency of defects of vertebral body formation by vertebral column level. For clarity, the unclassified vertebral malformations (n=35) were not included in this graph. Reprinted with permission from Gutierrez-Quintana et al. 2014.

3.3 Congenital thoracic vertebral malformation and neurological status

The dorsal and dorso-lateral hemivertebrae were only present in Group 1, and these were interpreted to be the cause of neurological deficits in 5/12 (41.6%) of these dogs. Butterfly and wedge shape vertebrae were identified in both groups, but were more commonly seen in Group 2 dogs with no neurological deficits (Table 4). In ten dogs with multiple congenital vertebral malformations, MRI studies confirmed that the butterfly vertebrae were not found to be the cause of the spinal cord compression, but another co-existing congenitally malformed vertebral was.

There was a statistically significant difference in the number of vertebral malformations between the dogs with associated neurological deficits and those without associated neurological deficits using the Fisher exact test ($P = 0.01$).

Vertebral malformation	All dogs	Group 1	Group 2
Block vertebra	1	1	0
Ventral aplasia of the vertebral body (Dorsal hemivertebra)	3	3	0
Ventro-lateral aplasia of the vertebral body (Dorso-lateral hemivertebra)	2	2	0
Lateral aplasia of the vertebral body (Lateral hemivertebra)	0	0	0
Ventral and median aplasia of the vertebral body (Butterfly vertebra)	24	4	20
Ventral hypoplasia of the vertebral body (Ventral wedge shape)	20	6	14
Lateral hypoplasia of the vertebral body (Lateral wedge shape)	0	0	0
Total number of vertebrae with a classified congenital malformation	50	16	34
Total number of vertebrae with an unclassified congenital malformation	35	14	21
Total number of vertebrae evaluated	362	154	208

Table 4 Number of vertebrae affected by each type of congenital vertebral malformation in dogs with associated neurological deficits (group 1) and dogs without associated neurological deficits (group 2). A significant difference in the types of congenital vertebral malformations was evident when comparing the two groups ($P = 0.01$) reprinted with permission from Gutierrez-Quintana et al. 2014.

3.4 Cobb angle measurement method assessment

A total of 37 vertebrae were identified and assessed twice by the 3 observers within the population of 28 dogs (37 vertebrae x 3 observers x 2 assessments= 222 angles were assessed).

The intra-and the inter-observer ICC were both excellent when assessing the Cobb angle to quantify spinal curvature on digital radiographs; when the confidence interval was set at 95% (CI 95%), it remained excellent. Table 5 outlines the intra- and inter-observer correlation coefficients for the Cobb angles and their 95% confidence intervals (CI).

	<i>Data</i>	<i>ICC</i>	<i>CI 95%</i>
Kyphosis	Intrarater1	0.996	0.992-0.998
	Intrarater2	0.989	0.980-0.995
	Intrarater3	0.984	0.969-0.992
	Interrater1,2,3	0.982	0.967-0.990
	Interrater1,2,3	0.972	0.950-0.985
	Cobb angles		
Scoliosis	Intrarater1	0.99	0.980-0.995
	Intrarater2	0.958	0.915-0.979
	Intrarater3	0.936	0.876-0.967
	Interrater1,2,3	0.957	0.926-0.976
	Interrater1,2,3	0.964	0.936-0.981

Table 5 Intraclass correlation coefficient (ICC) and 95% confidence intervals (CI) for digital measurement of the Cobb angles. 1,2,3: refer to the 3 observers reprinted with permission from Guevar et al. 2014.

3.5 Cobb angles, spinal deformity and neurological status

Data on the population and the neurological status are summarized in Table 2 and Table 3 (page 57). A flow chart explaining the analysed data sets is in the addendum.

The mean Cobb angle of all measured radiographs for kyphosis was 24.0° (n: 222; median: 16.9°; range: 0.0° -87.0°), and 5.69° for scoliosis (n: 222; median: 3.0°; range: 0° -49.7°). After selecting the highest kyphotic and scoliotic angles when multiple malformations were present, 9 sets of data were removed from the total number of angles (222 angles – (9 x 3 observers x 2 assessments= 56 angles) = 168 angles). The mean Cobb angle for kyphosis of the affected population was 45.6° (n: 72; median: 49.3°, range: 7.7° -87.0°) and 16.9° for the non-affected population (n: 96; median: 14.6°; range: 1.5° -47.9°). The mean Cobb angle for scoliosis of the affected population was 9.3° (n: 72; median: 4.1°; range 0.0° - 49.7°) and 3.8° (n: 96; median: 2.4°; range: 0° -17.6°) for the non-affected population.

There was a statistically significant difference between the kyphotic angles of the affected and the non-affected population ($P=0.0006$), but there was no statistically significant difference between the scoliotic angles of the 2 groups ($P=0.5462$).

A kyphotic angle greater than 35° had a positive predictive value of 75% for related neurological deficits (negative predictive value of 100%), with a sensitivity and specificity of 100% and 84% respectively (**Figure 27**, page 59).

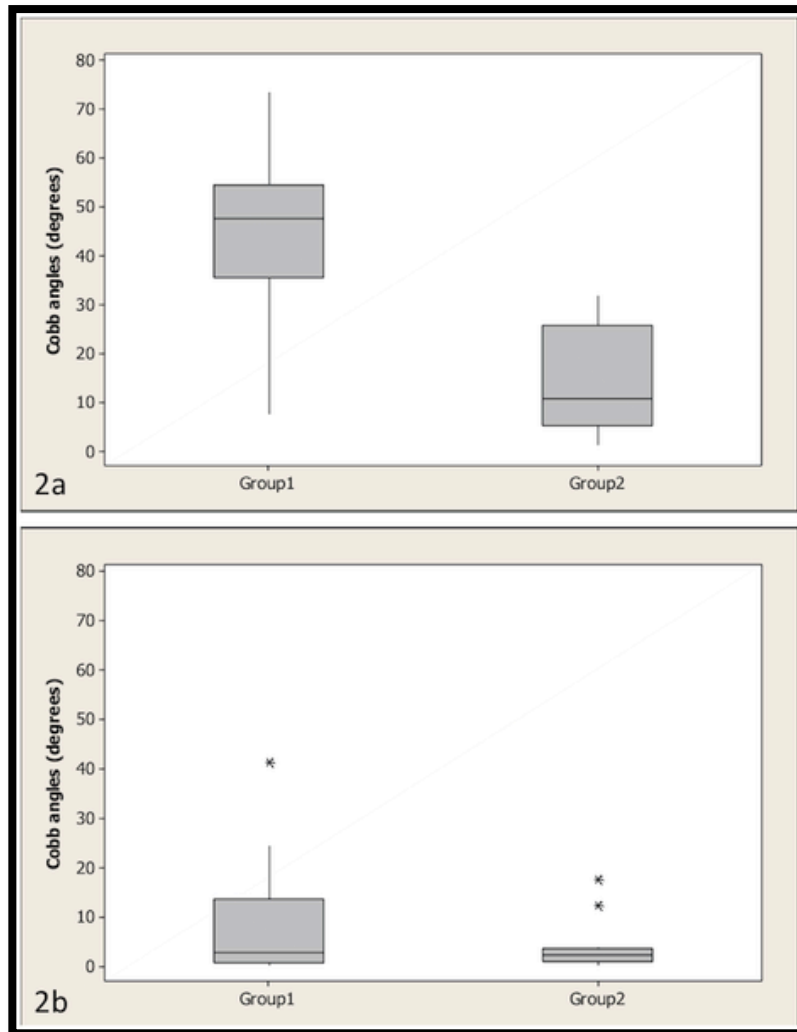


Figure 28 Boxplots of the kyphotic Cobb angles for group1 and group 2 (2a) ($P=0.0006$) and boxplots of the scoliotic angles of groups 1 and 2 (2b) ($P=0.5462$) reprinted with permission from Guevar et al. 2014.

4.1 Population and neurological status

The Pug breed was noted to have neurological deficits in 75% of the population studied. Two explanations are plausible for this over-representation of neurological deficits in this breed. The first one is that the breed may suffer from more severe vertebral malformations or, the second is that the breed is more common in our referral hospital population. Also, a majority (56%) of the English bulldogs presented with malformed vertebra without neurological deficits. Further studies with larger population are necessary to investigate the breed predispositions associated with these malformations.

The female and male population was equally represented. Although, the population size is small, with 6 individual in each group, this absence of evident sex predilection is in accord with other publication (Dewey et al. 2015).

When reviewing the age of the neurologically affected population, it appears that myelopathy secondary to vertebral malformations worsen at around 2 years of age (mean: 2.4y). The age at the time of clinical presentation is reported to be wide but dogs younger than a year old are reported to represent 60% of the population (Charalambous et al. 2014). The existence of a period of accelerated growth around 4-10 months of age (adolescence) has been suggested has a reason why these conditions, although present at birth are not clinically apparent until then (Westworth & Sturges 2010).

The population of dogs in this study is low and represent one of its limitations. However, it represents a hospital population over a period of 3.5 years and includes dogs with congenital thoracic vertebral malformations identified incidentally but also on neurological

work-ups. In this manner, a broad population without the bias for neurological deficits was targeted.

Another limitation resides in the distribution of breeds between the neurologically affected and non-affected groups being different and this could have influenced the type of vertebral malformations seen in each group. This again may be linked to the hospital population

4.2 Identification and classification of the congenital thoracic vertebral malformations

The findings of this work were consistent with the previous reports (Westworth & Sturges 2010; Dewey & da Costa 2016) indicating that congenital vertebral malformations are a common finding in the thoracic vertebral column of brachycephalic “screw-tailed” dog breeds, with 23.5% of the vertebrae examined in this study being affected.

The most commonly affected vertebra was in the midthoracic region (T6-T9 region), confirming previous reports (Volta et al. 2005; Westworth & Sturges 2010; Moissonnier et al. 2011). The majority of dogs with neurological signs (75%) presented with a chronic and progressive history of ambulatory paraparesis and ataxia (Grade 2), which suggested slowly progressive spinal cord injury and/or compression, consistent with previous reports (Aikawa et al. 2007; Jeffery et al. 2007; Westworth & Sturges 2010; Moissonnier et al. 2011;).

Multiple vertebral malformations were found to affect the majority of the dogs (64.2%). Again, this is a finding which corroborates well with other previous studies describing a

high frequency of vertebral abnormalities in French bulldogs, English bulldogs, and other brachycephalic breeds with multiple vertebrae commonly affected (Done et al. 1975; Volta et al. 2005; Moissonnier et al. 2011; Schlensker & Distl 2013).

A translated radiographic classification of congenital vertebral malformations was proposed and applied in dogs based on previous human studies which were assessing congenital kyphotic, scoliotic, and kypho-scoliotic malformations (Nasca et al. 1975; McMaster & Singh 1999). It was identified that applying this radiographic classification to dogs allowed inclusion of the majority of the different types of vertebral malformations present in these breeds, specifically the defects of vertebral body formation. Nonetheless, it was highlighted that 35 vertebral malformations failed to meet the classification criteria and that amongst those, 26 were judged as having a vertebral body of shorter length but with a normal shape. Therefore it is recommended that for future studies this type of defect of vertebral body formation should be added to the classification scheme under the term: symmetrical hypoplasia of the vertebral body (or “short” vertebra) (**Figure 29**). The residual nine vertebral malformations could not be included in any particular category based on radiography evaluation and the authors believe that for future studies, the use of advanced imaging may overcome this limitation of the classification system.

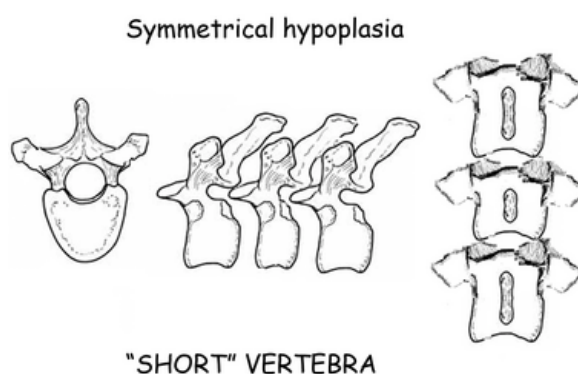


Figure 29 Schematic line drawings of the short vertebra: showing the radiographic appearance of the additional vertebral malformation found frequently in this study: symmetrical hypoplasia of the vertebral body (“short” vertebra) reprinted with permission from Gutierrez-Quintana et al. 2014.

It was also found that in this population of dogs the defects of vertebral formation were more common than the defects of vertebral segmentation. This is similar to what has previously been reported in the veterinary (Morgan 1968) and human literature (McMaster & Singh 1999).

Finally, another interesting finding was that no lateral aplasia or hypoplasia of the vertebral body was observed. This could well explain why kyphosis and kypho-scoliosis are more frequent and important than scoliosis in brachycephalic “screw-tailed” dog breeds.

4.3 Congenital thoracic vertebral malformations and neurological Status

Also in accord with the findings in human studies, it was identified that the severity of defects of vertebral body formation is related to the severity of the kyphosis (McMaster & Singh 1999). Indeed, more severe defects of vertebral body formation, including ventral and ventro-lateral aplasia of the vertebral body (dorsal and dorso-lateral hemivertebrae), were more likely to be associated with neurological deficits. Also, results indicated that the less severe vertebral body formation defects such as ventral and median aplasia (butterfly vertebra) or ventral hypoplasia of the vertebral body (ventral wedge shape vertebra) are common and can be seen in dogs with and without neurological deficits.

In two of the 12 cases with neurological deficits, it was found that the clinical signs were not a direct consequence of vertebral canal stenosis caused by the vertebral column deformity, but rather secondary to another neurological disease that occurred concurrently. In both cases, the intervertebral discs adjacent to the vertebral malformation were the focus of spinal cord involvement (one dog with Hansen type I intervertebral disc herniation and

the other dog with discospondylitis and secondary empyema). It is possible that intervertebral instability between the normal and malformed vertebrae could have resulted in damage to the intervertebral disc and predisposed it to herniation or infection. It has been indeed reported that congenital vertebral malformation results in early degeneration of adjacent intervertebral discs (Faller et al. 2014). Another study also reports the possible instability of the abnormal vertebral segment secondary to the vertebral malformations (Dewey et al. 2015).

4.4 Cobb angle measurement method assessment

Although the Cobb angle has been used previously in veterinary medicine to assess spinal deformities in dogs (Aikawa et al. 2007; Moissonnier et al. 2011; Aikawa et al. 2014; Charalambous et al. 2014), this study is the first report assessing the reliability of a computer-assisted digital radiographic measurement method to calculate the Cobb angle in the veterinary literature. Our results confirmed that the evaluation of the Cobb angle on digital radiographs is a feasible and reliable method to quantify the degree of spinal curvature in dogs.

It is believed that to be useful, the method would have to bear clinical value but also to be accessible, feasible and easily reproducible; the findings confirm that the technique regroups those three characteristics. The accessibility of the technique was achieved by using digital radiography, which is an imaging system commonly available and therefore accessible for veterinary practitioners. The research aimed to evaluate the feasibility and the reproducibility of the Cobb angle measurements via a computer assisted, commercially available plug-in for digital radiography analysis of patients with abnormal spinal curvatures. The feasibility was defined as successful placement of the Cobb angle lines.

The reproducibility was assessed by using the ICC. It was confirmed that this method was feasible and that its reproducibility was excellent, with ICC values over 0.9 (Shrout & Fleiss 1979; Fleiss 1986). When assessing the observation, with confidence interval set at 95%, the conclusion was that it remained excellent. By assessing this method on digitalized radiography, it would offer the advantage of evaluating a technique which is accessible for general practitioners, and where image size and contrast could be modulated to better define the vertebral end plates. Advanced imaging was not contemplated in this study as it was not judged appropriate to fulfil the criteria of ease of access.

Cobb angle measurements have been reported to have a high variability due to incorrect definition of the end vertebra, as well as defective angle measurement (Gstoettner et al. 2007). It is clear that inaccuracy in angle measurement exists and is inherent in the method itself. The measurement of a three-dimensional structure can only be attempted in a two-dimensional radiographic plane. In order to address these sources of error, a software plug-in that automatically calculates the Cobb angle and pre-defined end-vertebrae was used. Nonetheless, there was some degree of difficulty encountered in drawing a line through a vertebral end plate, which was not always evident as a straight line on the radiographs, as well as the difficulty in defining some of the vertebral endplates when vertebrae were superimposed, in particular on ventro-dorsal view radiographs. Good standard radiographic technique is still essential.

4.5 Cobb angles and neurological status

The finding that kyphosis is the main spinal deformity observed in this group of neurologically affected dogs and that a cut-off kyphotic angle exists around 35° supports

the fact that the degree of kyphosis secondary to the vertebral malformations determine the likelihood of developing neurologic dysfunction.

The potential of progression of congenital vertebral anomalies is unknown in dogs but has been highlighted in human literature, with careful assessment and monitoring being essential and early intervention may be desirable. In this context, potential healthy young dogs with a kyphotic angle below, but close to, 35° may benefit from monitoring for the subsequent appearance of neurological deficits. Serial Cobb angle measurements in these patients would also allow objective determination of progression of vertebral angulation facilitating early intervention. There is currently no supportive data to suggest any advantages for preventive stabilization with spinal surgery in dogs without neurological deficits; although early intervention may be warranted to prevent them.

Scoliosis is also identified in this population of dogs with a mean scoliotic angles for the 2 groups being lower than 10° and without substantial clinical impact. This latter finding corroborates with other reports in veterinary and human literature (McMaster & Singh 1999; Westworth & Sturges 2010).

The final limitation is the retrospective nature of this study. Retrospective studies are indeed recognised to have a number of limitations related to accurate record keeping, selection bias and misclassification bias (Sedgwick 2014).

4.6 Conclusions

By studying congenital vertebral malformations in a population of brachycephalic screw tailed dogs, several goals were achieved.

First of all, this work allowed adapting and defining a radiographic classification scheme for congenital vertebral malformations in dogs from human medicine. There is hope that the new classification which, by being clear and well-defined, will become a reference tool for veterinarians and help terminology to be more conventionally applied on the topic of congenital vertebral malformations.

Second, this research allowed the description of which congenital vertebral malformations were more frequently identified and, most importantly, which ones were more likely to lead to neurological deficits. Kyphosis was subsequently identified as the most common vertebral deformity occurring secondary to the congenital vertebral malformations. With this data, it was then possible to conclude that within a population of brachycephalic screw tailed dog breeds, dogs with kyphosis were more likely to suffer from neurological deficits.

Third, the research aimed to study the relationship between vertebral column curvatures and dogs neurological status. For that purpose, it was therefore elected to adapt a new method of calculation of the Cobb angle, which is the gold standard measurement for these conditions in human. The new method was reliable and reproducible and there is hope that this last characteristic will help to disseminate the use of this technique and assist in quantifying curvature of vertebral column deformities in dogs. A cut-off angle above which a dog was more likely to develop neurological deficits was also determined.

Validating this technique enabled to study vertebral column deformities (kyphosis and scoliosis) and to confirm that the population affected with neurological deficits had a greater Cobb angle. The severity of kyphotic deformity was related with the clinical presentation.

The radiographic scheme and vertebral column deformity calculation method are 2 new tools of reference that could be routinely applied by veterinarians in both general practice and referral centres to evaluate congenital vertebral malformations and their potential consequences in brachycephalic “screw-tailed” dogs.

LIST OF REFERENCES

1. Dewey C, da Costa R. Myelopathies: disorders of the spinal cord. In: Dewey C, da costa R, eds. *A Practical Guide to Canine and Feline Neurology*. 3rd ed. Wiley-Blackwell; 2016:329-403.
2. Westworth DR, Sturges BK. Congenital spinal malformations in small animals. *Vet Clin North Am Small Anim Pract*. 2010;40(5):951-981.
3. Dewey CW, Davies E, Bouma JL. Kyphosis and Kyphoscoliosis Associated with Congenital Malformations of the Thoracic Vertebral Bodies in Dogs. *Vet Clin North Am Small Anim Pract*. 46.2 (2016): 295-306.
4. Schlensker E, Distl O. Heritability of hemivertebrae in the French bulldog using an animal threshold model. *Vet J*. 2016;207:188-189.
5. Alexander PG, Tuan RS. Role of environmental factors in axial skeletal dysmorphogenesis. *Birth Defects Res Part C - Embryo Today Rev*. 2010;90(2):118-132.
6. Kaplan KM, Spivak JM, Bendo JA. Embryology of the spine and associated congenital abnormalities. *Spine J*. 2005;5(5):564-576.
7. Fleming A, Keynes R, Tannahill D. A central role for the notochord in vertebral patterning. *Development*. 2004;131(4):873-880.
8. Mead TJ, Yutzey KE. Notch signaling and the developing skeleton. *Adv Exp Med Biol*. 2012;727:114-130.
9. Vosbikian MM, Petfield JL, Lawrence JP, et al. Spinal embryology and anatomy of the pediatric spine. In: Vaccaro AR., Fehlings MG., Dvorak MF, eds. *Spine and Spinal Cord Trauma: Evidence-Based Management*. Thieme medical publishers; 2011:39-50.
10. Carlson BM. Development of the body systems. In: *Human Embryology and Developmental Biology*. Philadelphia, Pa. Mosby/Elsevier; 2014:156-178.
11. Nolting D, Hansen BF, Keeling J, et al. Prenatal development of the normal human vertebral corpora in different segments of the spine. *Spine*. 1998; 23(21): 2265-2271.
12. Summers BA, Cummings JF, Delahunta A. Malformations of the central nervous system. In: Summers BA, Cummings JF, Delahunta A, eds. *Veterinary Neuropathology*. St Louis, MO: Mosby; 1995:68-94.
13. Chesney C. A case of spina bifida in a Chihuahua. *Vet Rec*. 1973;93(5):120-121.
14. Arias MV, Marcasso RA, Margalho FN, et al.. Spina bifida in three dogs. *Braz J Vet Pathol*. 2008;1(2):64-69.
15. Shamir M, Johnston D, Rochkind S. Surgical treatment of tethered spinal cord syndrome in a dog with myelomeningocele. *Vet Rec*. 2001:755-756.
16. Clayton H, Boyd J. Spina bifida in a German shepherd puppy. *Vet Rec*. 1983;112(1):13-15.
17. Frye FL, Mcfarland LZ. Spina bifida with rachischisis in a kitten. *J Am Vet Med Assoc*. 1965;146:481-482.
18. Ricci E, Cherubini GB, Jakovljevic S, et al. MRI findings, surgical treatment and follow-up of a myelomeningocele with tethered spinal cord syndrome in a cat. *J*

Feline Med Surg. 2011;13(6):467-472.

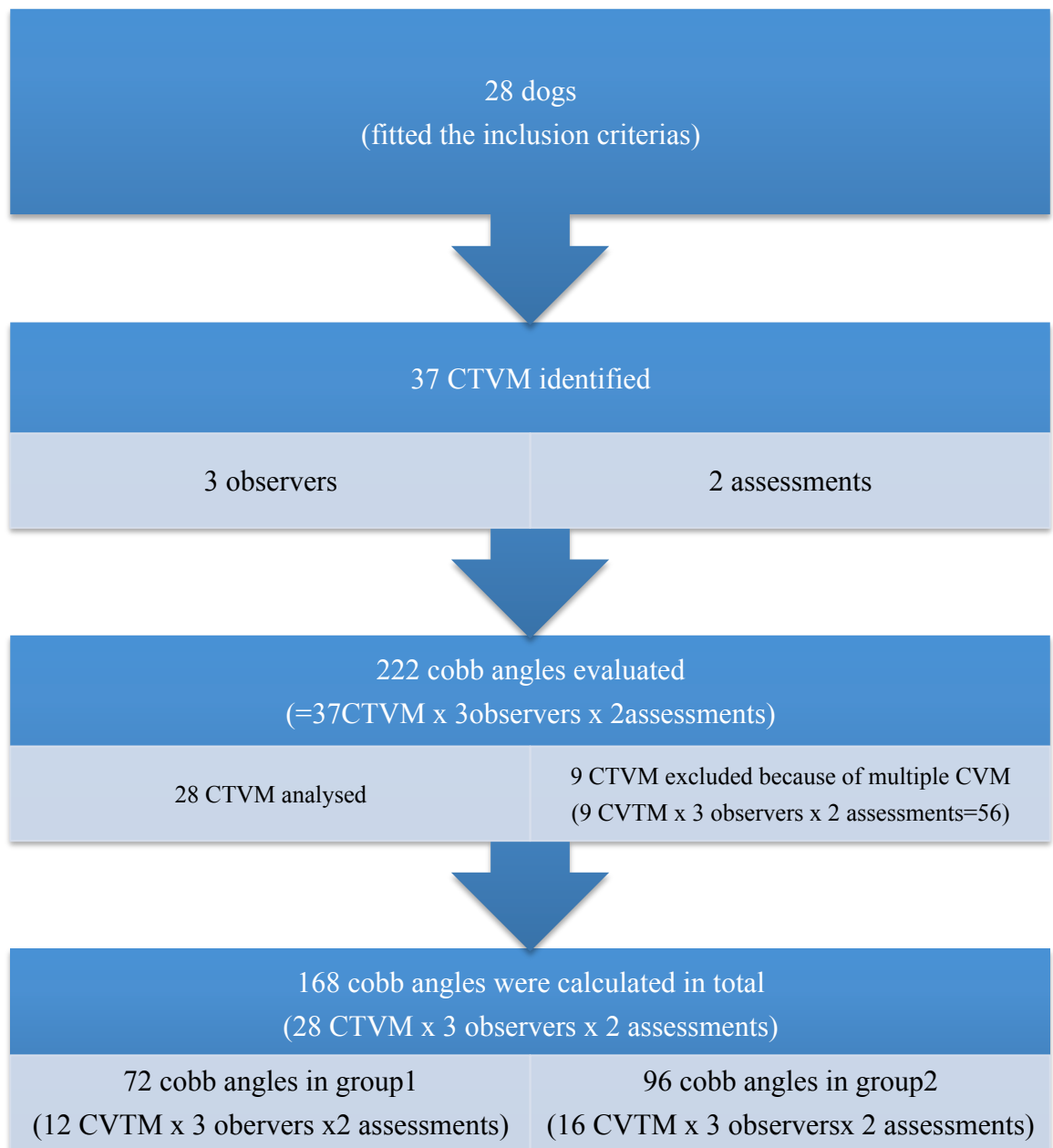
19. James CC, Lassman LP, Tomlinson BE. Congenital anomalies of the lower spine and spinal cord in Manx cats. *J Pathol.* 1969;97(2):269-276.
20. Martin AH. A Congenital Defect in the Spinal Cord of the Manx Cat. *Vet Pathol.* 1971;8(3):232-238.
21. Deforest ME, Basrur PK. Malformations and the Manx syndrome in cats. *Can Vet J.* 1979;20(11):304-314.
22. Newitt A, German AJ, Barr FJ. Congenital abnormalities of the feline vertebral column. *Vet Radiol Ultrasound.* 2008;49(1):35-41.
23. Robinson R. Expressivity of the Manx Gene in Cats. *J Hered.* 1993;84(3):170-172.
24. Pretzer SD. Canine embryonic and fetal development: A review. *Theriogenology.* 2008;70(3):300-303.
25. Tsou PM, Yau A, Hodgson AR. Embryogenesis and prenatal development of congenital vertebral anomalies and their classification. *Clin Orthop Relat Res.* 1980;(152):211-231.
26. Morgan JP. Congenital Anomalies of the Vertebral Column of the Dog: A Study of the Incidence and Significance Based on a Radiographic and Morphologic Study1. *Vet Radiol.* 1968;9(1):21-29.
27. Grenn HH, Lindo DE. Hemivertebrae with severe kypho-scoliosis and accompanying deformities in a dog. *Can Vet journal.* 1969;10(8):214-216.
28. Malik Y, Konar M, Wernick M, et al. Chronic intervertebral disk herniation associated with fused vertebrae treated by vertebral lateral corpectomy in a cat. *Vet Comp Orthop Traumatol.* 2009;22(2):170-173.
29. Kramer JW, Schiffer SP, Sande RD, et al. Characterization of heritable thoracic hemivertebra of the German shorthaired pointer. *J Am Vet Med Assoc.* 1982;181(8):814-815.
30. Mazrier H, Van Hoesen M, Wang P, et al. Inheritance, Biochemical Abnormalities, and Clinical Features of Feline Mucopolidosis II: The First Animal Model of Human I-Cell Disease. *J Hered.* 2003;94(5):363-373.
31. Jaskwhich D, Ali RM, Patel TC, et al. Congenital scoliosis. *Curr Opin Pediatr.* 2000;12(1):61-66.
32. Nasca RJ, Stilling FH, Stell HH. Progression of congenital scoliosis due to hemivertebrae and hemivertebrae with bars. *J Bone Jt Surgery.* 1975;57(4):456-466.
33. McMaster MJ, Singh H. Natural history of congenital kyphosis and kyphoscoliosis. A study of one hundred and twelve patients. *J bone Jt surgery.* 1999;81(10):1367-1383.
34. Volta A, Morgan JP, Gnudi G, et al.. Clinical-radiological study of the vertebral abnormalities in the english bulldogs. In: *Proceeding of the 12th Annual Conference of the European Association of Veterinary Diagnostic Imaging.* Naples; 2005:31.
35. Besalti O, Ozak A, Pekcan Z, et al. Nasca classification of hemivertebra in five dogs. *Ir Vet J.* 2005;58(12):688-690.
36. Kealy JK, McAllister H, Graham JP. The skull and vertebral column. In: Saunders, ed. *Diagnostic Radiology and Ultrasonography of the Dog and Cat.* 5th ed. St Louis.: Elsevier Health Sciences; 2011:447-541.
37. Moissonnier P, Gossot P, Scotti S. Thoracic kyphosis associated with hemivertebra.

- Vet Surg.* 2011;40(8):1029-1032.
38. Aikawa T, Shibata M, Asano M, et al. A comparison of thoracolumbar intervertebral disc extrusion in French Bulldogs and Dachshunds and association with congenital vertebral anomalies. *Vet Surg.* 2014;43(3):301-307.
 39. Cobb J. Outline for the study of scoliosis. In: *Am Acad Orthop Surg Instr Course Lect.* 1948;261-275.
 40. Langensiepen S, Semler O, Sobottke R, et al. Measuring procedures to determine the Cobb angle in idiopathic scoliosis: a systematic review. *Eur Spine J.* 2013;22(11):2360-2371.
 41. Srinivasalu S, Modi HN, Smehta S, et al. Cobb angle measurement of scoliosis using computer measurement of digitally acquired radiographs-intraobserver and interobserver variability. *Asian Spine J.* 2008;2(2):90-93.
 42. Tanure MC, Pinheiro AP, Oliveira AS. Reliability assessment of Cobb angle measurements using manual and digital methods. *Spine J.* 2010;10(9):769-774.
 43. Zhang J, Lou E, Hill DL, et al. Computer-aided assessment of scoliosis on posteroanterior radiographs. *Med Biol Eng Comput.* 2010;48(2):185-195.
 44. Qiao J, Liu Z, Xu L, et al. Reliability analysis of a smartphone-aided measurement method for the Cobb angle of scoliosis. *J Spinal Disord Tech.* 2012;25:E88-E92.
 45. Morrissy RT, Goldsmith GS, Hall EC, et al. Measurement of the Cobb angle on radiographs of patients who have scoliosis. Evaluation of intrinsic error. *J Bone Jt Surgery.* 1990;72(3):320-327.
 46. Polly D, Kilkelly F, McHale K. Measurement of lumbar lordosis: evaluation of intraobserver, interobserver, and technique variability. *Spine.* 1996;21(13):1530-1535.
 47. Kuklo T, Polly D, Owens B. Measurement of thoracic and lumbar fracture kyphosis: evaluation of intraobserver, interobserver, and technique variability. *Spine.* 2001;26(1):61-66.
 48. Keynan O, Fisher C, Vaccaro A, et al. Radiographic measurement parameters in thoracolumbar fractures: a systematic review and consensus statement of the spine trauma study group. *Spine.* 2006;31(5):E156-E165.
 49. Jeffery ND, Smith PM, Talbot CE. Imaging findings and surgical treatment of hemivertebrae in three dogs. *J Am Vet Med Assoc.* 2007;230:532–536.
 50. Aikawa T, Kanazono S, Yoshigae Y, et al. Vertebral stabilization using positively threaded profile pins and polymethylmethacrylate, with or without laminectomy, for spinal canal stenosis and vertebral instability caused by congenital thoracic vertebral anomalies. *Vet Surg.* 2007;36(5):432-441.
 51. McMaster MJ, Singh H. The surgical management of congenital kyphosis and kyphoscoliosis. *Spine.* 2001;26(19):2146-2154.
 52. Winter R. Neurologic safety in spinal deformity surgery. *Spine.* 1997;22(13):1527-1533.
 53. Charalambous M, Jeffery ND, Smith PM, et al. Surgical treatment of dorsal hemivertebrae associated with kyphosis by spinal segmental stabilisation, with or without decompression. *Vet J.* 2014;202(2):267-273.
 54. Sharp NJ, Wheeler SJ. Thoracolumbar disc disease. In: *Small Animal Spinal Disorders: Diagnosis and Surgery.* Elsevier Mosby; 2005:121–159.
 55. Gutierrez-Quintana R, Guevar J, Stalin C, et al. a Proposed Radiographic

Classification Scheme for Congenital Thoracic Vertebral Malformations in Brachycephalic “Screw-Tailed” Dog Breeds. *Vet Radiol Ultrasound*. 2014;55(6):585-591.

56. Shrout P, Fleiss J. Intraclass correlations: uses in assessing rater reliability. *Psychol Bull*. 1979;86:420-428.
57. Fleiss J. Reliability of Measurement. In: *The Design and Analysis of Clinical Experiments*. Toronto: Wiley; 1986:1-32.
58. Guevar J, Penderis J, Faller K, et al. Computer-assisted radiographic calculation of spinal curvature in brachycephalic “screw-tailed” dog breeds with congenital thoracic vertebral malformations: reliability and clinical evaluation. *PLoS One*. 2014;9(9):e106957.
59. Done S, Drew R, Robins G, et al. Hemivertebra in the dog: clinical and pathological observations. *Vet Rec*. 1975;96(14):313-317.
60. Schlensker E, Distl O. Prevalence, grading and genetics of hemivertebrae in dogs. *Eur J Companion Anim Pract*. 2013;23:119–123.
61. Faller K, Penderis J, Stalin C, et al. The effect of kyphoscoliosis on intervertebral disc degeneration in dogs. *Vet J*. 2014;200(3):449-451.
62. Gstoettner M, Sekyra K, Walochnik N. Inter-and intraobserver reliability assessment of the Cobb angle: manual versus digital measurement tools. *Eur Spine J*. 2007;16:1587-1592.
63. Sedgwick P. Retrospective cohort studies: advantages and disadvantages. *BMJ*. 2014;348:g1072.

Addendum:



Addendum 1: Flow chart explaining the selection of congenital thoracic vertebral malformations (CTVM) and the numbers of cobb angle assessed within the population for the study of cobb angles in brachycephalic screw tailed dogs.